University of West Bohemia
Faculty of Applied Sciences
Department of Cybernetics

MASTER'S THESIS

Characterisation of off-target activation in cell-cell signal transmission networks

Pilsen 2016 Hynek Kasl

Prohlášení

Předkládám tímto k posouzení a obhajobě diplomovou práci zpracovanou na závěr studia na Fakultě aplikovaných věd Západočeské univerzity v Plzni.

Prohlašuji, že jsem diplomovou práci vypracoval samostatně a výhradně s použitím odborné literatury a pramenů, jejichž úplný seznam je její součástí.

V Plzni dne 12. května

. . . . . .

Declaration

I hereby declare that this master thesis is completely my own work and that I used only the cited sources.

Acknowledgment

I would like to express my sincere gratitude to my advisor M.Sc. Daniel Georgiev, PhD for his unconditional support, enlightened advice and brilliant supervision.

Abstrakt

Studium mezibuněčné komunikace je důležitou oblastí biologie. Důmyslně navržené komunikační sítě lze nalézt v organismech od bakterií po savce. Přesto není moc známo o způsobu jejich návrhu. Tato práce uvádí novou metodu modelování zaměřenou na optimalizaci těchto sítí. Navržená metoda je použita při optimalizaci tří biologicky odlišných případů jednokrokové homogenní komunikační sítě. Je ukázáno, že použití pozitivní zpětné vazby je výhodné pro rychlou a přesnou komunikaci. Nastavení síly zpětné vazby je dále diskutováno. Získané výsledky jsou porovnány s příklady použití zpětné vazby v bakteriálních quorum sensing sítích.

Klíčová slova: mezibuněčná komunikace, matematické modelování, optimalizace, pravidla návrhu, kladná zpětná vazba

Abstract

Intercellular communication is an important field of study in biology. Intricately designed communication networks are found in organisms ranging from bacteria to mammals, yet not much is known about the design behind them. This work proposes a novel modelling method focused on optimization of communication networks. The proposed method is used to optimize the performance of a one-step communication network, with three biologically different cases considered. It is shown that designs utilizing positive feedback yield the best performance, and the feedback setup is discussed. A biological parallel to the derived results is found in the use of positive feedback in bacterial quorum sensing.

Keywords: intercellular communication, mathematical modelling, design optimization, design rules, positive feedback

Contents

List of Figures

1. Introduction

Complex communication networks are well known in biology, and are found in many life-forms, ranging from bacteria to higher organisms. These networks have a very broad range of functions, e.g., cell cycle synchronization, developmental signaling, and social patterns creation, and employ various communication molecules, e.g., small organic molecules and peptides. However the underlying mechanisms, including positive and negative feedback, are often similar between different organisms, communication functions, and communication means. Bacterial quorum sensing networks presented in Chapter [2] are a class of communication networks that were excessively studied from a biological perspective. These networks are widely used in bacteria for various tasks, such as biofilm formation, and often utilize positive feedback, yet not much is known toward their optimal design.

It is often the case that the native communication networks are relatively complex and therefore models used to simulate them are often complex as well, and limited to numerical solution only. In this work a method that produces analytic models of communication networks focused on optimization is developed. The method is based on several assumptions that limit its applicability to signalling among co-localized cells. In Chapter [3], the method is described more thoroughly and a model of homogeneous single marker one step activation model.

The models derived using the method offer strong options for optimization. This is demonstrated on the example model derived in Chapter [3]. Firstly, the definition of network performance is studied and an applicable metric is proposed. Secondly, three biologically different cases of the model are considered, and the design rules that yield the optimal performance are derived. It is shown that using positive feedback in communication is beneficial toward network performance, and the optimal feedback set-up is discussed. Obtained results are shown to be in agreement with positive feedback utilization in some quorum sensing networks.

2. Biological Motivation

2.1 Cell-cell communication

Intercellular communication is a vast area of interest in modern biology. More or less all organisms, except for viruses, use communication to interact with other organisms in the surrounding environment. Recently, intercellular communication has been employed and studied even in genetically modified organisms. It is of course desired to learn as much as possible about the native communication systems to exploit that knowledge for synthetic systems.

Unfortunately, it is often difficult to decide why native communication networks were designed so. The communication systems, especially in higher, multicellular organisms, are often largely interlinked with other biological processes inside the cells and other communication systems. Therefore not many of the systems are completely known, even though the involved networks are an important focus of study, and new surprising data emerge every year. Additionally, even lower life forms, such as bacteria exhibit complex cell-cell signalling, with a vast range of functions.

2.2 Target recognition

In this work, we focus on target recognition by co-localized cells, a special subclass of cell-cell communication with a specific purpose. Co-localized cells are cells attached to a biological entity in close proximity to each other. Cells then use communication to make a group decision to activate based on the identity of the entity the are attached to, i.e., target recognition. More specifically, cells want to activate if the entity is the target (on-site activation) and minimize activation elsewhere (off-site activation). It is presumed that a decision made by a group is in some way better than that made by a single cell. Cells that recognize the target will be referred to as sensor cells. Target can be recognized from background by its specific biological surface marker(s). In a real world scenario, sensor cells will need to recognize the target among other entities that don't have the target marker (background). Even though cells display antibody (fragments) that are complementary to the target specific marker(s), realistically sensor cells could possibly form bonds, albeit weak, with background. To minimize the chance of off-site activation, sensor cell communication network must be carefully designed.

Even though target recognition by sensor cells is widespread , e.g. recognition of pathogens by immune system, and has even spread to genetically modified systems (iGEM 2015 IOD Band `http://2015.igem.org/Team:`

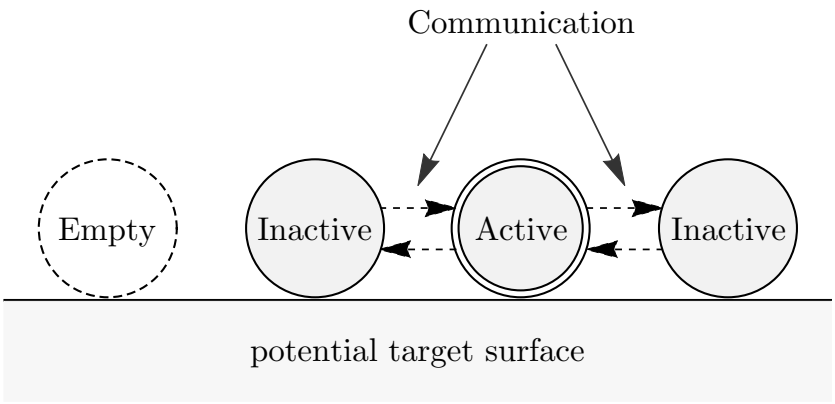

Figure 2.1: Communication between colocalized cells

`Czech_Republic`), in this work we focus on quorum sensing triggered biofilm formation to study the communication design. Quorum sensing, a class of bacterial communication networks, are relatively smaller in the number of communication molecules, proteins, and genes involved, yet some of the mechanisms that drive them are similar to that of multicellular organisms. Quorum sensing networks are also well characterized in many of the current model bacteria. That makes them an excellent example to study from a network design point-of-view.

2.3 Biofilm formation

Bacteria are often thought of as isolated organisms, yet many species are highly social and often live in communities. Some bacteria prefer community life even in favorable locations, while others revert to social life only as a response to stress. Inside these communities, bacteria communicate, exchange DNA and resources, change their environment by expressing extracellular proteins, etc. Once inside a community, the cell's behavior often changes drastically, including gene expression patterns. Furthermore, even the community may have different states, based on its size and local physical (flow, temperature), chemical (pH, nutrients), and biological (competitors, predators) stresses.

One type of these communities is a biofilm. The formation of a biofilm occurs in several stages. Firstly, a few bacterii attach to the target surface. If the conditions are right, the number of bound bacterii increases, and once a threshold is reached, expression of extracellular matrix proteins begins. This pushes the number of bacterii even higher, till a steady state is reached,

when the natural growth and death to stresses are balanced. Afterwards, the biofilm survives until external conditions change, and parts of the biofilm may fall of to form biofilms elsewhere. Note that many of the involved processes happen at very different time-scales, with diffusion and flow being the fastest and protein expression being the slowest. This suggests that approximations such as time-scale separation are used in modelling of such systems. Biofilms can also be created by different species acting in symbiosis. Even biofilms created by a single species have cells in different states, corresponding to the cell's location inside the biofilm. That is, biofilms are often formed in layers, where different layers have different expression patterns and behave differently (e.g. aerobic and anaerobic layers). The expression pattern changes that are vital to biofilm formation and survival, occur several times during its development, and are triggered by the quorum sensing communication networks. Genes expressed in the various community states of a cell are useless to a cell that is alone, and incorrect activation of their expression would be detrimental.

2.4 Quorum sensing

Quorum sensing (QS) is a name for a diverse set of communication networks found in bacteria. The common characteristic of all QS systems is the expression, secretion and sensing of communication molecules by all cells to respond to changes in local cell density and adjust their behavior accordingly [1]. From a control theory point-of-view, quorum sensing system acts as an internal bacterial estimator of the surrounding cells location and density. QS systems use two different types of molecules, both of which are produced intracellularly. The first type are small organic molecules called acyl homoserine lactoses (AHLs) and are used by Gram-negative bacteria. Smaller AHL are often highly diffusible which enables them free transfer trough the cell membrane. Larger AHLs are actively transported outside the cell by membrane pumps. The second type are smaller (though larger than AHLs) peptides used by Gram positive bacteria [2]. These are also actively transported outside by transporters. The detection is also different for each molecule type. AHLs are mostly transported inside where they bind to cytoplasmatic regulator proteins (such as *LuxR* in *Vibrio Fischeri*) [3]. The cytoplasmatic regulator-AHL complex then alters gene transcription pattern. Some AHLs and peptides bind to membrane receptors that trigger a phosphorylation cascade inside, which activates a transcription factor that changes gene expression pattern. This is somewhat similar to phosphorylation cascades in eukaryotes, such the yeast pheromone pathway. Different signalling molecule concentrations may lead to different responses. One molecule can

therefore be used to alter gene expression more times, e.g. once the cells enter logarithmic stage and once they enter stationary phase. Furthermore, a single species may use more than one QS system to alter expression of different genes separately or at different cell densities (e.g. *Vibrio Fischeri* which employs *ain* QS system largely linked to colonization and *lux* system linked to fluorescence). Note that interspecies QS system also exist and some species intentionally invade communication channels of other species. An interesting prevalent feature of many QS system is autoinduction. Even though the communication molecules are expressed constitutively, their expression is often further increased by sensing of the communication molecule. This positive feedback loop is found in many of the QS systems which hints at its importance in communication [4].

Interestingly, the positive feedback strength and utilization varies between different species and even between different networks in a single species (e.g. *Bacillus subtilis* [5]). Additionally, even in networks that have similar functions (such as virulence factor expression or biofilm formation in pathogenic bacteria), the balance between constitutive expression and positive feedback expression differs. The purpose of these differences is not yet fully explained. The networks' biochemical setups are usually qualitavely known, but quantitave information (e.g. reaction rates) is still unknown [6].

This work investigates the use of positive feedback in quorum sensing triggered biofilm formation through a model of a basic quorum sensing system that utilizes positive feedback. Biologically different cases of the model are optimized to yield the best performance. The optimal set-up is then studied w.r.t. desired activation properties. An interesting link between the desired activation density and feedback strength is found. This link is further examined in Chapter [5] and is used to explain the differences in feedback strength in pathogenic bacteria.

3. Modelling

3.1 Introduction

Currently, there are many different approaches to modelling of intercellular communication, as there are many things to be considered, e.g., cell spatial distribution, producion, diffusion, degradation of the communication molecules, and many other biological processes inside the cells. On a whole, a model that considers all of the above mentioned processes would be too complex to provide any intuition into the network design whatsoever. Hence, various approximations were proposed to reduce the model complexity and obtain useful results. Usually, the problem is reduced by assuming simple spatial and time distributions of the cells, such as a stationary cells. From the various modelling methods, the most complex are agent based models that model each cell (agent) independently and the model the the whole system as a combination of its agents. Such models can include most of the above mentioned processes [7] [8] however are limited to numerical solutions only. A well known class of such models are cellular automata. Such models replace agents with a lattice and a set of discrete transition rules. Even simple rules then enable simulation of complex systems [9] [10] though numerical only. A different approach is to describe the communication processes directly through a set of biochemical and physical equations. Then, a combination of partial differential equations, that account for diffusion and degradation, and ordinary differential equations, that account for other biological processes is used. Such models are often used to show spatial patterns and social behavior [11] [12]. Such models may in theory be solved analytically, but in practice are often limited to numerical modeling of an already existing communication systems. Models are also created by combining the above mentioned methods creating so-called hybrid models.

In this work, a **new method** for the modelling of communication between co-localized cells is developed. The method and the modelled system are described below.

3.2 General Network Model

3.2.1 Model and Basic Facts

Suppose that there is a population of cells, referred to as sensor cells, that use communication to activate at a desired spot, referred to as the target, and never activate anywhere else, referred to as background. The whole population of sensor cells and their communication network is referred to as the sensor system. The target may be a rare cell or other biological entity,

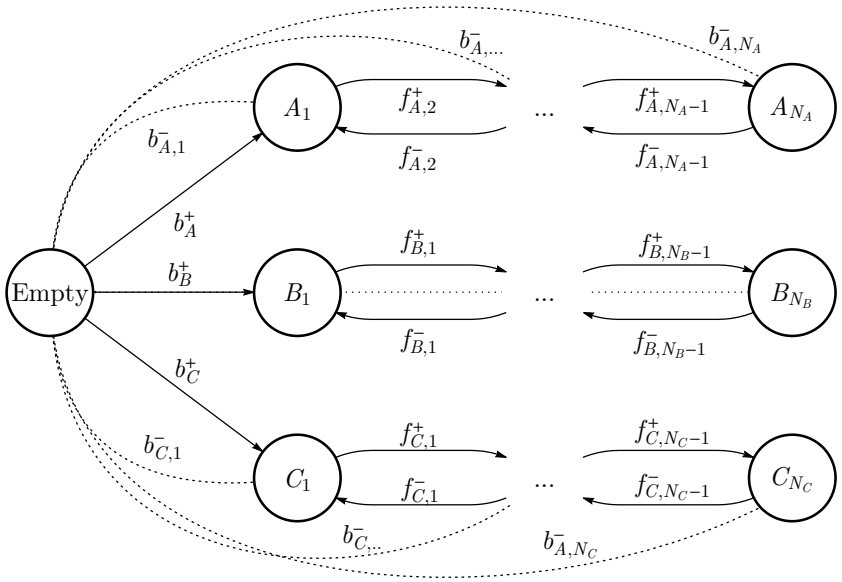

Figure 3.1: An illustration of possible states of one binding site a in a general model along with transitions between them.

and is recognizable from other biological material by its characteristic surface markers. A general sensor system comprises of sensor cells of different types, denoted by letters, and each cell type X has N_X different levels of activation, denoted by arabic numerals. One of activation levels (typically the last) of one of the cell types is the overall output of the sensor system. Once a cell of this type reaches its last activation level a biological change is triggered, e.g., agglutination, an immune response, etc.

The construction of a model of the sensor system activation is described below. We assume that the communication between the cells is only local, and once a sensor cell is bound (potential target), it can only influence sensor cells bound nearby. This assumption is substantiated by the often high degradation rate of native communication molecules, sometimes even actively increased by expression of enzymes that degrade the communication molecule by communicating cells [13]. Then, on each point r of the surface (of the potential target) in time t a cell type X in activation state i may be bound with probability $p_{X,i}(r,t)$ where

$$X \in \{0 \cup \{A, B, \cdots\}\}$$
$$i \in [1, 2, \cdots, N_X]$$

where 0 denotes the empty state, which has one level of activation (none). Possible states are shown in Figure [3.1]

Naturally, it must hold that each point r is in one of these states at any time t, i.e., the sum of these probabilities is always

$$\forall t, r \sum_{X \in A,B,\cdots} \sum_{i=1}^{N_X} p_{X,i}(r,t) = 1$$

We can then describe the transitions between the states at any point r and at any time t by a stochastic process continuous in time and discrete in states. Such a process is described by the Kolmogorov forward equation

$$\frac{dp(r,t)}{dt} = F\left(p(r,t)\right) p(r,t) \tag{3.1}$$

where $F\left(p(r,t)\right)$ is a general transition function. We assume a homogeneous medium such that transitions occur with equal probability anywhere, i.e., F is not a function of r. To simplify the model further, we omit the spatial information altogether by focusing on binding sites in homogeneous areas such that $p(r,t) = p(t)\ \forall r$. For example, during the formation of a biofilm, the binding spots on the target far from the edge are roughly equal, and start from the same state (empty), and can therefore be described by the same transition function

$$F\left(p(r,t)\right) = F\left(p(t)\right). \tag{3.2}$$

This does not hold for binding spots near the edge of the target, where communication occurs differently from beyond the boundary.

Note that the transition rate is dependent on time through $p(t)$. The sensor system detects the presence of the target, a rare cell. The sensor cells cannot bind to something that isn't there, therefore we can assume that the whole surface of the cell starts in the empty state, mathematically

$$p(0) = [p_0(0), p_{A,1}(0), \cdots]^{\mathrm{T}} = \left[1, 0, \cdots\right]^{\mathrm{T}} = e_1^{\mathrm{T}} \tag{3.3}$$

The whole system is therefore described as

$$\frac{dp(t)}{dt} = F(p(t))p(t) \qquad p(0) = e_1 \tag{3.4}$$

Fundamentally, there are four important types of transitions for each cell type. These are

Name	Transition	Rate
Association of X	$0 \to X_1$	$b_X^+(p(t))$
Dissociation of X_i	$X_i \to 0$	$b_{X,i}^-(p(t))$
Activation of X_i	$X_i \to X_{i+1}$	$f_{X,i}^+(p(t))$
Deactivation of X_i	$X_i \to X_{i-1}$	$f_{X,i}^-(p(t))$

To illustrate how the transition rates translate into the transition function we consider the association transition. This transition leads from an empty state to type X 1-active state, i.e., for the association of type X, we add

$$\begin{aligned}\frac{dp_0(t)}{dt} &= \cdots - b_X^+(p(t))p_0(t)\cdots \\ \frac{dp_{X,1}(t)}{dt} &= \cdots + b_X^+(p(t))p_0(t)\cdots\end{aligned}$$

where $b_X^+(p(t))$ is the association rate of type X. The other transitions are described by similar relations. Note that even though one cell type is assumed to recognize one marker, different activation states of that type do not need to have the same dissociation rate to that marker. The dissociation rate can be tuned by, e.g., the number of antibodies displayed on the sensor cell surface.

3.2.2 Homogeneous population model

In the simplest case, the sensor system comprises of a single type of sensor cells. These cells recognize a single marker, however may have different dissociation rates toward that marker. The last activation state N is considered as the output. The possible states of the surface are then and the system is then described by the following system of equations

$$\begin{aligned}\frac{dp_0}{dt} &= -b^+p_0 + \sum_{i=1}^{N+1} b_i^- p_i, \\ \frac{dp_1}{dt} &= +b^+p_0 - (b_1^- + f_1^+)p_1 + f_1^- p_2, \\ \frac{dp_i}{dt} &= +f_{i-1}^+ p_{i-1} - (b_i^- + f_i^+ + f_i^-)p_i + f_{i+1}^- p_{i+1}, \\ &\vdots \\ \frac{dp_N}{dt} &= +f_{N-1}^+ p_{N-1} - f_N^- p_N - b_N^- p_N.\end{aligned}$$

Note that the rates may be dependent on $p_1, p_2, \ldots, p_N$. By laws of probability, it always holds that

$$\sum_{i=0}^{N} p_i = 1.$$

Below, this model will be used as a stepping stone towards a one-step activation model in Section [3.3.2], design of which is the main focus of this work.

3.3 One Step Activation Model

3.3.1 Problem Definition

The main focus of this work is the design optimization of a homogeneous one step activation model derived in this section. Biologically, one step activation is defined as follows

Definition I: One step activation

One step activation is a communication protocol where a sensor cell is activated after sensing a signal from another sensor cell, which is produced independently of previous communication. Only two levels of activity, active and inactive, are then sufficient.

The surface can therefore be in one of following three states

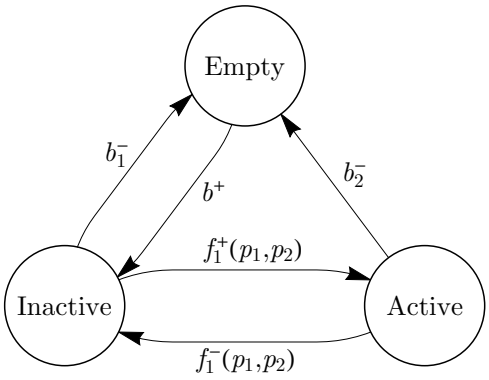

State	Probability
Empty	$p_0(t)$
Inactive	$p_1(t)$
Active	$p_2(t)$

Rate of	Notation
association	$b^+(p_1, p_2)$
dissociation 1	b_1^-
dissociation 2	b_2^-
activation	$f^+(p_1, p_2)$
deactivation	$f^-(p_1, p_2)$

The general system is described by the following ordinary differential equations

$$\begin{aligned}
\frac{dp_0}{dt} &= -b^+(p_1,p_2)p_0 + b_1^- p_1 + b_2^- p_2, \\
\frac{dp_1}{dt} &= +b^+(p_1,p_2)p_0 - b_1^- p_1 - f^+(p_1,p_2)p_1 + f^-(p_1,p_2)p_2, \\
\frac{dp_2}{dt} &= +f^+(p_1,p_2)p_1 - f^-(p_1,p_2)p_2 - b_2^- p_2,
\end{aligned} \tag{3.5}$$

The binding has to always be in one of these states, therefore it always holds that

$$p_0(t) + p_1(t) + p_2(t) = 1 \quad \forall t \in [0;\infty].$$

3.3.2 Model Reduction

To develop a biologically relevant one step activation model, several assumptions are made. These assumptions are

1	Association rate is constant and independent of current state $$b^+ \neq b^+(p, T) = const.$$
2	Affinity towards markers doesn't change with activation $$b_2^- = b_1^-$$
3	Association is much faster than activation $$T(t) = T_\infty = const.$$
4	Activation rate is increased linearly by p_1 and p_2 $$f^+(p_1, p_2) = a^+ + w_1 p_1 + w_2 p_2$$
5	Deactivation rate is constant and independent of p_1 and p_2 $$f^- = a^- \neq f^-(p_1, p_2) \geq 0$$

Below, these assumptions are described in more detail and with biological justification and context. The impact of each assumption on the model is discussed.

Assumption 1

Association rate is constant and independent of current state

$$b^+ \neq b^+(p_1, p_2) = const.$$

Context

To change the association rates of nearby sensor cells, an already bound sensor cell would either need to influence the production of antibodies in other nearby sensor cells or directly produce and send them antibodies. However, antibody related processes occur on a completely different time scale than intercellular communication. Whereas communication occurs on a timescale of minutes, production, folding and displaying of antibodies on snesor cell surface usually takes hours, perhaps even more, and is very costly for the cells resource wise. Extracellular transport would take even more time and resources and perhaps even not be possible at all. Controlling the association rate is therefore non-viable strategy if results are expected in short time [hours]. Besides, the relation between the association rate and probabilities p_1, p_2 would be very difficult to specify.

Assumption 2

Sensor cell affinity towards markers doesn't change after activation

$$b_2^- = b_1^- = b^-$$

Context

To change its dissociation rate after becoming active, the sensor cell would need to alter the concentration of antibodies on its surface. As was mentioned in Assumption [2], antibody related processes occur on a completely different time scale than intercellular communication. Whereas communication occurs on a timescale of minutes, production, folding and displaying antibodies on a membrane usually takes hours, perhaps even more, and is very costly for the cells resource wise. Controlling the dissociation rate of active sensor cells is therefore a non-viable strategy if results are expected in hours. Besides, the relation between the dissociation rate and antibody production/concentration would be difficult to specify.

Under these two assumptions, the system is then described by the following system of three first order differential equations

$$\frac{dp_0}{dt} = -b^+ p_0 + b^- p_1 + b^- p_2, \tag{3.6}$$

$$\frac{dp_1}{dt} = +b^+ p_0 - b^- p_1 - f^+(p_1, p_2)p_1 + f^-(p_1, p_2)p_2, \tag{3.7}$$

$$\frac{dp_2}{dt} = +f^+(p_1, p_2)p_1 - f^-(p_1, p_2)p_2 - b^- p_2, \tag{3.8}$$

A new variable can be defined that reduces the system order by one. Let

$$T(t) = p_1(t) + p_2(t) = 1 - p_0(t) \tag{3.9}$$

be the probability that either an active or an inactive sensor cell is bound. Then

$$\frac{T(t)}{dt} = b^+ - (b^- + b^+)T(t) \quad \text{with} \quad T(0) = 0.$$

Equation [3.7] is no longer needed as the probability of an inactive sensor cell $p_1(t)$ bound can be computed at any time as $p_1(t) = T(t) - p_2(t)$. Equation [3.8] takes the form of

$$\frac{dp_2(t)}{dt} = + f^+(T, p_2)(T - p_2) - f^-(T, p_2)p_2 - b^- p_2. \tag{3.10}$$

The system can therefore be described by the following set of two ordinary differential equations.

(3.11)

Assumption 3

Association is much faster than activation, therefore $T(t)$ can be assumed constant

$$T(t) = T_\infty = const. \tag{3.12}$$

Context

In difference to binding, which usually occurs on the order of seconds, activation is based on communication and transcription/translation systems, which take from minutes to hours to activate. Additionally, communication itself is dependent on diffusion of the communication molecule, which itself takes seconds.

Under this assumption, the originally time dependent variable $T(t)$ is replaced by its steady state value T_∞

$$T_\infty = \lim_{t\to\infty} T(t) = \frac{b^+}{b^+ + b^-}. \tag{3.13}$$

The system then takes the form of one algebraic and one first order differential equation.

$$\frac{dp_2(t)}{dt} = + f^+(T_\infty, p_2)(T_\infty - p_2) - f^-(T_\infty, p_2)p_2 - b^- p_2. \tag{3.14}$$

If the activation rate $f^+(T_\infty, p_2)$ or the deactivation rate $f^-(T_\infty, p_2)$ is a function of p_2 then the differential equation is non-linear in the unknown value $p_2(t)$ and therefore problematic to solve. Below, the time solution of the general one step model in Equation [3.16] is derived. The steady state probability of active state

$$\lim_{t\to\infty} p_2(t) = p_\infty \tag{3.15}$$

shall be referred to as the steady state activity p_∞. Below we shall not consider probabilities of empty state $p_0(t)$ and inactive state $p_1(t)$, therefore we shall refer to $p_2(t)$ simply as $p(t)$.

3.3.3 Case Studies Introduction

To specify the problem, we need to specify the activation and deactivation function.

Assumption 4

Activation rate is affinely dependent on the probabilities of active and inactive sensor cell

$$f^+(p_1, p_2) = a^+ + w_1 p_1 + w_2 p_2$$

Context

An affine function serves as a first step towards solving a more complicated relationship. This represents a cell that reacts linearly to the concentration of the communication molecule. Note that this may not be the best way to model as native cells usually employ an all-or-nothing response to communication molecule concentration. The system is however analytically unsolvable with such a response.

Initially, a similar assumption, albeit with affine decrease instead of increase, was placed on the deactivation rate $f^-(p_1, p_2)$. The system was still solvable, however unfortunately, the solution took many different forms based on the optimization and their meaning was difficult to physically interpret. Therefore we set $f^-(p_1, p_2) = a^-$. Then

$$\begin{aligned}\frac{dp_2(t)}{dt} &= +(a^+ + w_1 T_\infty)T_\infty - (a^+ + a^- + b^- + 2w_1 T_\infty - w_2 T_\infty)p_2 \\ &\quad - (w_2 - w_1)p_2^2. \end{aligned} \tag{3.16}$$

This differential is quadratic in the unknown value $p_2(t)$. Below, three biologically relevant cases of the one step activation problem are defined.

Definition II: Spontaneous activation

Spontaneous activation is defined as activation where no communication occurs.

$$w_1 = w_2 = 0$$

The activation is then defined only by the basal rate a^+. This is the simplest of the cases, both mathematically and biologically. Sensor cells produce no communication molecule, and bound sensor cells become active independently of any communication from their surroundings. Note that the activation half-time is $\frac{1}{a^+}$.

Definition III: Constitutive activation

Constitutive activation is defined as activation where inactive and active communication occurs, and both active and inactive sensor cells activate neighbors with equal propensity.

$$w_1 = w_2 = w > 0$$

The activation is then defined by the basal rate a^+ and the communication rate w. In this case, both active and inactive sensor cells produce a communication molecule with equal rate. This communication molecule is then sensed by neighboring inactive sensor cells, and their rate of activation is affinely increased.

Definition IV: Induced activation

Induced activation is defined as activation where inactive and active communication occurs, and active and inactive sensor cells activate neighbors with different propensity.

$$w_1 \geq 0 \wedge w_2 \geq 0 \wedge w_1 \neq w_2$$

The activation is then defined by the basal rate a^+, the communication rate of inactive cells w_1 and the communication rate of active cells w_2. Similar to constitutive activation, both active and inactive sensor cells produce a communication molecule. However, the production rate is different between active and inactive cells, i.e., activation also changes the production rate of the molecule. This may be done as a feedback activation of the communication molecule gene, i.e., w_2 can be thought of as feedback activation rate. The molecule is then sensed by neighboring inactive sensor cells, and their probability of activation is increased.

3.3.4 System Solution

Consider a general first order quadratic differential equation

$$\frac{dp(t)}{dt} = ap(t)^2 + bp(t) + c \quad \text{with} \quad p(0) \tag{3.17}$$

Equation [3.17] represents the one step activation model (Equation [3.16]), derived in previous Section [3.3.2], if

$$\begin{aligned} a &= -(w_2 - w_1) \\ b &= -(b^- + a^+ + 2w_1T_\infty - w_2T_\infty + a^-) \\ c &= (a^+ + w_1T_\infty)T_\infty \end{aligned}$$

By solving this quadratic differential equation, we solve the general one step activation in time. The time solution of this nonlinear equation is different for $a = 0$ and for $a \neq 0$.

Linear Case

The simplest case is when $a = 0$, which is satisfied if $w_2 = w_1$ in Equation [3.16], which holds for spontaneous and constitutive activation. In this case the non-linear differential equation [3.17] reduces to the following linear differential equation

$$\frac{dp}{dt} = bp(t) + c.$$

The time solution of this equation is given as

$$p(t) = -\frac{c}{b}\left(1 - e^{bt}\right). \tag{3.18}$$

We see that the solution converges only if $b \leq 0$. The steady state value is then

$$p_\infty = \lim_{t\to\infty} p(t) = -\frac{c}{b}. \tag{3.19}$$

The time solution may therefore be rewritten as

$$p(t) = p_\infty\left(1 - e^{bt}\right). \tag{3.20}$$

Nonlinear Case

In case $a \neq 0$, which is satisfied if $w_2 \neq w_1$, i.e., induced activation in the general one step activation model, the differential equation stays non-linear. However, the equation is still solvable through the following state space transformation. One can define the error from the steady state $\epsilon(t)$ as

$$\epsilon(t) = p(t) - p_\infty, \tag{3.21}$$

where p_∞ is the stable steady state given by

$$ap_\infty^2 + bp_\infty + c = 0 \rightarrow p_\infty = -\frac{b}{2a} \pm \frac{1}{2a}\sqrt{b^2 - 4ac} \tag{3.22}$$

For the stable steady state, it must hold that

$$\frac{d}{dp}(ap^2 + bp + c)\Big|_{p=p_\infty} = 2ap_\infty + b < 0$$

Since $\sqrt{b^2 - 4ac} \geq 0$, the stable steady state is

$$p_\infty = -\frac{b}{2a} - \frac{1}{2a}\sqrt{b^2 - 4ac}. \tag{3.23}$$

It will be useful to also introduce the complementary unstable steady state

$$p^*_\infty = -\frac{b}{2a} + \frac{1}{2a}\sqrt{b^2 - 4ac}. \tag{3.24}$$

Since $\epsilon(t)$ is $p(t)$ shifted by a term constant in time then by substitution, we derive

$$\frac{dp(t)}{dt} = \frac{d\epsilon(t)}{dt} = a\epsilon(t)^2 + (b + 2ap_\infty)\epsilon(t) \tag{3.25}$$

with the initial condition

$$\epsilon(0) = -p_\infty.$$

We have obtained a quadratic differential equation without the constant term. Such an equation is solvable with the following nonlinear transformation of the state space

$$\epsilon(t) = \frac{1}{\xi(t)} \tag{3.26}$$

$$\frac{d\epsilon(t)}{dt} = -\frac{1}{\xi(t)^2}\frac{d\xi(t)}{dt} \tag{3.27}$$

By substitution, we derive

$$\frac{d\xi(t)}{dt} = -a - (b + 2ap_\infty)\xi(t), \tag{3.28}$$

which reduced the nonlinear equation to a linear equation with initial condition

$$\xi(0) = \frac{1}{\epsilon(0)} = \frac{1}{p(0) - p_\infty} = -\frac{1}{p_\infty}. \tag{3.29}$$

We have therefore used exact linearization to obtain a solvable differential equation, whose solution is

$$\xi(t) = \frac{a}{b'} - \left(\frac{a}{b'} - \xi(0)\right)\exp\left[b't\right]. \tag{3.30}$$

where

$$b' = -b - 2ap_\infty = \sqrt{b^2 - 4ac} = a\left(p^*_\infty - p_\infty\right). \tag{3.31}$$

One can then rewrite Equation [3.30] as

$$\xi(t) = -\frac{p_\infty - p^*_\infty \exp\left[b't\right]}{(p_\infty - p^*_\infty)p_\infty} \tag{3.32}$$

From Equation [3.32], we can obtain the solution of the original Equation [3.16]

$$p(t) = p_\infty + \epsilon(t) = p_\infty + \frac{1}{\xi(t)} = \\ = \left(1 - \frac{p_\infty - p^*_\infty}{p_\infty - p^*_\infty e^{b't}}\right) p_\infty. \tag{3.33}$$

Thus we obtained the full time solution to the general one step activation without.

4. Design optimization

4.1 Problem Definition

Sensor cells can be designed many different ways, with each of the designs possessing a set of tuneable parameters. The performance of each of these designs can be measured by a metric and parameter setups that yield the best performance can be found. However, the performance metric has to be specified first. Below, two performance metrics are described more thoroughly. Firstly, it is the minimization of false positives. It is shown that this metric provides useful results in mathematically simpler cases, yet provides unnatural results leading to infinite activation times in more complicated and biologically interesting cases. Secondly a different metric is proposed, which uses activation time as the criterion with constraints on both false negatives and false positives. Application of this metric is then shown on three biologically relevant cases homogeneous one step activation model derived in previous Chapter.

4.2 Minimization of False Positives

The activity can be qualitatively measured by the stationary probability of active sensor cell. It is desired that this probability is close to one on target and close to zero elsewhere. Medically, the impact of incorrect activation at one of the background cells, i.e., a false positive, is worse as it can lead to, e.g., misdiagnosis of cancer, however, non-activation at one of the targeted cells, i.e., a false negative, is also desired to be minimized.

The system performance can be measured by, e.g., the probability of false positives and the probability of false negatives. The probabilities are computed as follows. To model the different bond strengths between sensor cells and targets, and between sensor cells and background, it can be assumed that the association rate is constant for all bonds while the dissociation rate is small for bonds between sensor cells and targets and very large for bonds between sensor cells and background. More rigorously, let the dissociation rate of sensor cell-target bonds be described by a random variable b^-_{target} with unknown probability distribution $p(\hat{b}^-_{\text{target}}, \sigma^2_{\text{target}})$, and the dissociation rate of sensor cell-background bonds by a random variable $b^-_{\text{background}}$ with unspecified probability distribution $p(\hat{b}^-_{\text{background}}, \sigma^2_{\text{background}})$. Identifying these distributions is difficult and experimentally tedious. Furthermore, it is likely the target cells will be present in much smaller concentrations than the background . Let the apriori probability that a cell is target cell be P_T and the apriori probability that it is background cell be $1 - P_T$. The total probability

of false negatives F_N is then

$$\begin{aligned} F_N &= P(\text{not active}|\text{target})P(\text{target}) \\ &= (1 - P(\text{active}|\text{target}))P_T \\ &= \left(1 - \int_0^\infty p(\text{active}|b^-_{\text{target}})p(b^-_{\text{target}})db^-_{\text{target}}\right) P_T. \end{aligned}$$

The probability of activation $p(\text{active}|b^-_{\text{target}})$ is considered as the steady state activity p_∞, therefore

$$F_N = (1 - E\left[p_\infty(b^-_{\text{target}})\right])P_T. \tag{4.1}$$

And similarly, the probability of false positives can be computed as

$$\begin{aligned} F_P &= P(\text{active}|\text{background})P(\text{background}) \\ &= \left(\int_0^\infty p(\text{active}|b^-_{\text{background}})p(b^-_{\text{background}})\text{d}b^-_{\text{background}}\right)(1 - P_T) \\ &= E\left[p_\infty(b^-_{\text{background}})|b^-_{\text{background}}\right](1 - P_T). \end{aligned} \tag{4.2}$$

To evaluate these expected values, knowledge of probability distributions $p(\hat{b}^-_{\text{target}}, \sigma^2_{\text{target}})$ and $p(\hat{b}^-_{\text{background}}, \sigma^2_{\text{background}})$ is needed. However, identifying these distributions would be difficult and experimentally tedious and perhaps not even possible by current available experimental methods. Instead, two point estimations are made, that reduce the needed knowledge of target and background dissociation rate distributions to single values. Illustration of the problem is shown on Figure [4.2].

Compared to background, where antibodies can bind to many different structures, target cells are covered by a known and well characterized marker, who mostly keeps its structure and surface concentration. The distribution of background dissociation rate $b^-_{\text{background}}$ therefore has a very high variance and very high difference between its lowest and highest possible value, which is the direct opposite of the target distribution. Mathematically, variance and higher moments of $p(\hat{b}^-_{\text{target}}, \sigma^2_{\text{target}})$ are insignificant, therefore $E[p_\infty(b^-_{\text{target}})]$ can be well approximated by the first term of its Taylor series

$$E[f(X)] \approx f(E[X]) + \frac{1}{2}f''\left(E[X]\right)E^2[X]$$

which yields

$$E[p_\infty(b^-_{\text{target}})] = p_\infty(E[b^-_{\text{target}}]) = p_\infty(\hat{b}^-_{\text{target}}). \tag{4.3}$$

For the sake of brevity, $\hat{b}^-_{\text{target}}$ will be referred to as b^-_T.

Unfortunately, similar assumption cannot be made about $b^-_{\text{background}}$. However, one can assume that the function $p_\infty(b^-_{\text{background}})$ is strongly decreasing in $b^-_{\text{background}}$. Therefore, an upper bound can be placed on $E[p_\infty(b^-_{\text{background}})]$ as

$$E[p_\infty(b^-_{\text{background}})] \leq p_\infty(b^-_B)(b^-_{\text{background}} - b^-_{\text{background},min}), \tag{4.4}$$

where b^-_B is the dissociation rate with maximal probability of false activation

$$b^-_B = \underset{b^-_{\text{background}}}{\arg\max}\, p_\infty(b^-_{\text{background}})p(b^-_{\text{background}}). \tag{4.5}$$

The value can be approximated from known background entites, chosen as the mean dissociation rate of the most common background entity or determined heuristically. Naturally, the value of b^-_B should always be larger than b^-_T, otherwise the problem is ill posed. Under these assumptions, the probability of false positives and the probability of false negatives is computed as

$$F_N = (1 - p_\infty(b^-_T))P_T, \tag{4.6}$$
$$F_P = p_\infty(b^-_B)(1 - P_T). \tag{4.7}$$

We see that both F_N and F_P are affine in the steady state activity p_∞ at target and at background, respectively. Further on, it will be useful to consider the steady state activity at target $p_\infty(b^-_T)$ instead of chance of false negatives F_N and the steady state activity at background $p_\infty(b^-_B)$ instead of chance of false positives.

Unfortunately $p_\infty(b^-_T)$ and $p_\infty(b^-_B)$ are not independent, and it can be shown that by reducing $p_\infty(b^-_B)$ one also decreases $p_\infty(b^-_T)$ therefore increasing F_N and vice versa, which is illustrated on Figure [4.2], suggesting that a balance has to be found between target and background steady state activity. The user has to specify how much false positive probability will be given up for lower false negative probability. Even though these performance metrics are not independently minimizable, as many of these designs have more than one free parameter, a constraint can be added such that designs considered in minimization keep equal steady state activity at target.

$$p_\infty(b^-_T) = 1 - \frac{F_N}{P_T} = c_N. \tag{4.8}$$

This approach was found to be useful in one class of problems , namely in problems that lead to linear systems, i.e., spontaneous and constitutive activation. Unfortunately, this approach provides unrealistic (and therefore useless) results in mathematically more class of problems, such as induced activation and dissociation rate changes. An example from each class is given

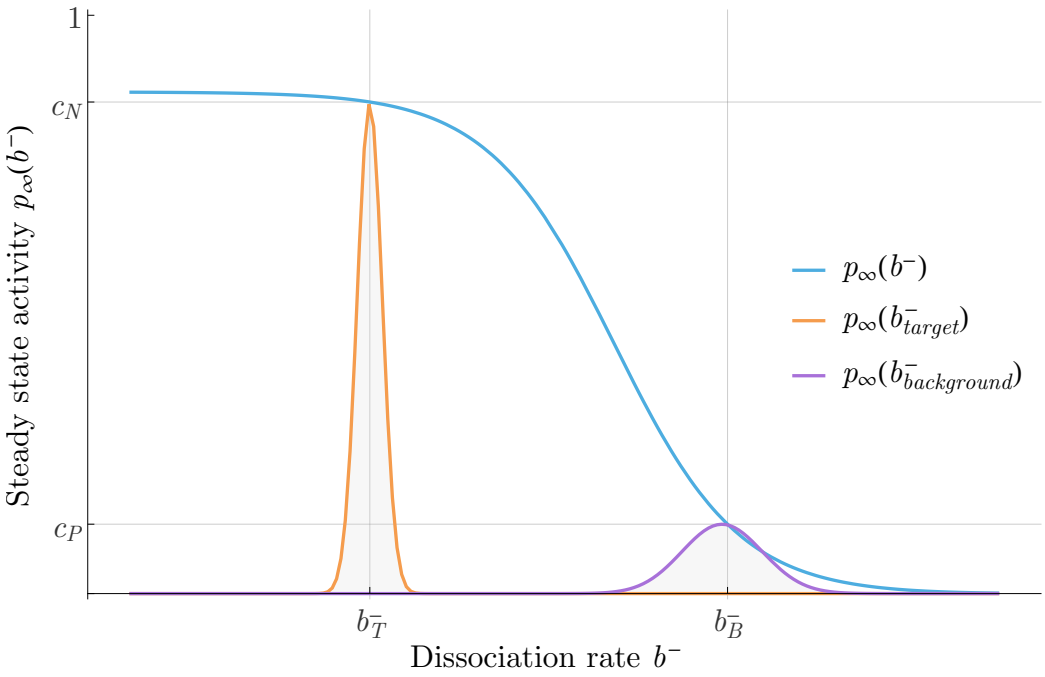

Figure 4.1: An example of steady state activity $p_\infty(b^-)$ as a function of b^- and possible distributions of b^-_{target} and $b^-_{background}$

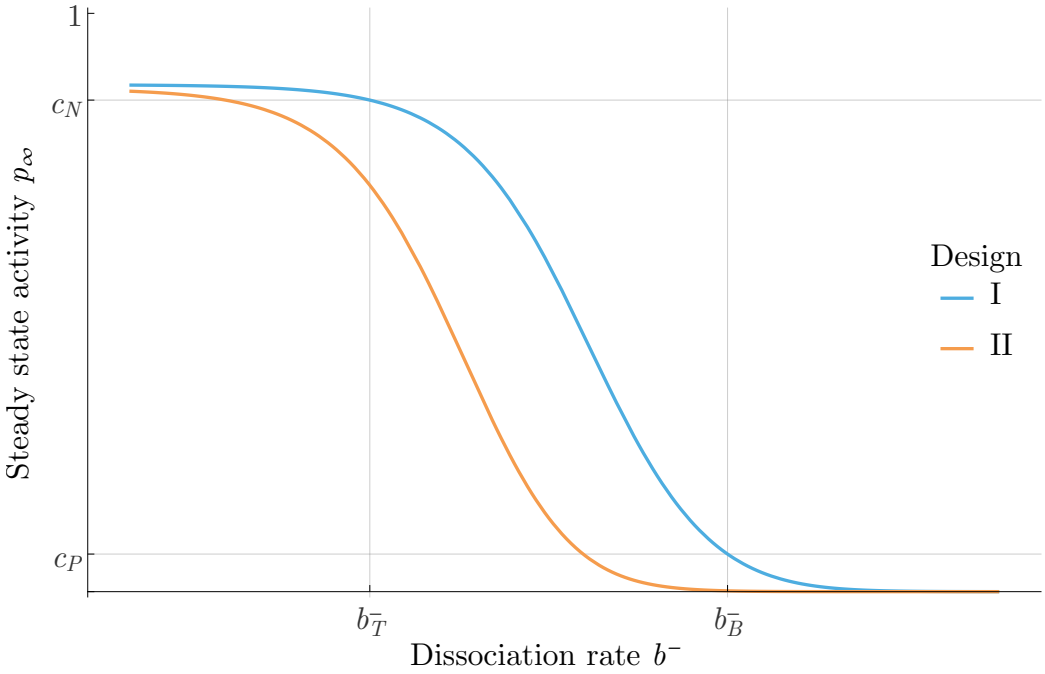

Figure 4.2: Problems of unconstrained minimization of false negatives.

below.

To simplify the computations in the following chapters, it is useful to introduce the probability of a bound sensor cell at target as

$$T_T = T_\infty\Big|_{b^-=b_T^-} = \frac{b^+}{b^+ + b_T^-},$$

and the probability of bound sensor cell at background as

$$T_B = T_\infty\Big|_{b^-=\Delta b_T^-} = \frac{b^+}{b^+ + \Delta b_T^-},$$

and ratios between the probability of active and inactive states at target , and at background respectively, as

$$\Gamma_N = \frac{P(\text{active}|\text{target})}{P(\text{inactive}|\text{target})} = \frac{c_N}{T_T - c_N}, \tag{4.9}$$

$$\Gamma_P = \frac{P(\text{active}|\text{background})}{P(\text{inactive}|\text{background})} = \frac{c_P}{T_B - c_P}. \tag{4.10}$$

Note that for the computations below, Γ_N fully replaces c_N and Γ_P fully replaces c_P. Most of the results obtained below are not expressed in terms of c_P and c_N because of their complexity.

4.2.1 Spontaneous Activation

An example of a problem where constrained minimization of false positives gives useful results is spontaneous activation case. Under spontaneous activation, Equation [3.16] reduces to a linear first order differential equation

$$\frac{dp(t)}{dt} = a^+ T_\infty - (a^+ + a^- + b^-)p(t) \quad p(0) = 0. \tag{4.11}$$

In constrained minimization of false positives, we are not interested in the time-related properties of Equation [4.11] and instead focus only on its steady value, which is given as

$$p_\infty = \frac{a^+}{a^+ + a^- + b^-} T_\infty \tag{4.12}$$

Spontaneous activation offers two tuneable parameters, which are a^+ and a^-, both of which are greater than or equal to zero. As was mentioned previously, if we were to minimize the probability of false positives, that is the steady state activity at background

$$J = p_\infty(\Delta b_T^-) = \frac{a^+}{a^+ + a^- + \Delta b_T^-} T_B. \tag{4.13}$$

We could, e.g., let $a^- \to \infty$ and then $\lim_{a^- \to \infty} J = 0$, therefore we would obtain zero rate of false positives. However, this would also result in $\lim_{a^- \to \infty} p(b_T^-) = 0$, therefore we would no correct activation on target either, i.e., a 100 percent chance of false negatives. We see that minimization of false positives alone results in increase of false negatives, as was mentioned above. To solve this, we have to add a constraint on the steady state activity at target, such that the compared designs have equal chance of false negatives

$$p_\infty(b_T^-) = \frac{a^+}{a^+ + a^- + b_T^-} T_T = c_N \tag{4.14}$$

Solving Equation [4.14] for a^+

$$a^+ = \frac{c_N}{T_T - c_N} a^- + b_T^- = \Gamma_N a^- + b_T^-. \tag{4.15}$$

Naturally, it must hold that $a^+ \geq 0$, which is true for any $a^- \geq 0$. After substitution of a^+ from Equation [4.15] back into the criterion

$$\begin{aligned} J &= \frac{\Gamma_N}{\Gamma_N + 1} \frac{a^- + b_T^-}{a^- + b_T^- + \frac{\Delta - 1}{\Gamma_N + 1} b_T^-} = \\ &= \frac{\Gamma_N}{\Gamma_N + 1} \left(1 - \frac{\frac{\Delta - 1}{\Gamma_N + 1} b_T^-}{a^- + b_T^- + \frac{\Delta - 1}{\Gamma_N + 1} b_T^-} \right). \end{aligned} \tag{4.16}$$

It can be seen that J in Equation [4.16] is a strictly increasing function of a^- for $a^- \geq 0$, therefore to minimize J, one needs to set a^- to its lowest possible value, which is $a^- = 0$. The optimal solution is therefore

$$\begin{aligned} a^+ &= \Gamma_N b_T^-, \\ a^- &= 0, \\ J &= \frac{\Gamma_N}{\Gamma_N + \Delta}. \end{aligned}$$

The Figure [4.3] below illustrates the difference in steady state activity curves for different rates of deactivation. The blue curve corresponds to the optimal solution, when $a^- = 0$. The orange curve corresponds to non-zero deactivation a^-. Note that there also exist a limiting solution as $a^- \to \infty$, which is given by

$$\lim_{a^- \to \infty} p = \frac{\Gamma_N}{\Gamma_N + 1} \frac{b^+}{b^+ + b^-} = \frac{c_N}{T_T} \frac{b^+}{b^+ + b^-} = c_N \frac{b^+ + b_T^-}{b^+ + b^-}.$$

This limiting solution is purely mathematical as it leads to infinite values of both a^+ and a^-, however is shown as the grey dashed line for completeness.

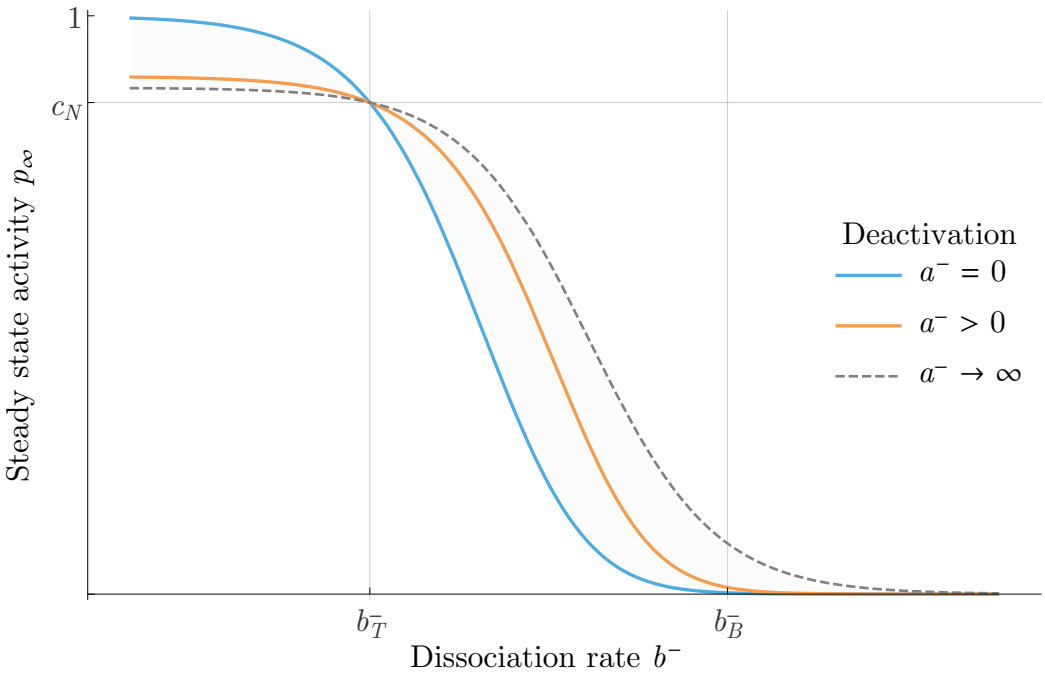

Figure 4.3: Impact of deactivation rate a^- on the steady state activity p_∞ as a function of b^- for spontaneous activation with a constraint on false negatives.

4.2.2 Induced Activation

An example of a problem where constrained minimization of false positives doesn't give useful results is the induced activation case.

$$\frac{dp(t)}{dt} = (a^+ + w_1 T_\infty)T - (b^- + a^+ + 2w_1 T_\infty - w_2 T_\infty + a^-)p(t) + (-w_2 + w_1)p^2(t)$$

with a constrain on false negatives

$$0 = (a^+ + w_1 T_T)T_T - (b_T^- + a^+ + 2w_1 T_T - w_2 T_T + a^-)c_N - (w_2 - w_1)c_N^2.$$

It can be shown that the criterion is strongly increasing in w_1 if we take the constraint into account. The proof is very tedious and was done using Mathematica software [14]. This means that to minimize false positives, we need to lower the initial rate of activation to 0+. In turn, the second activation rate $w_2 \to \infty$. Under these conditions $\lim_{w_1 \to 0+} J = 0+$. In this setting, the system takes infinitely long to activate a single sensor cell, but once it appears, all cells immediately activate to satisfy the constraints. This

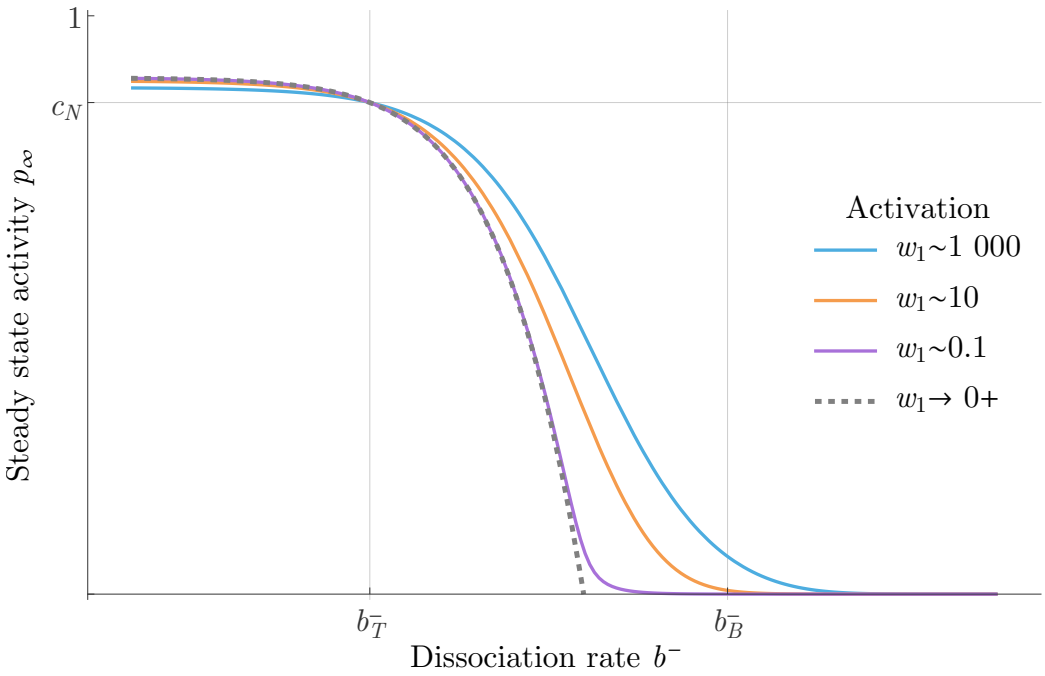

Figure 4.4: Impact of activation rate w_1 on the steady state activity p_∞ as a function of b^- for induced activation with a constraint on false negatives.

is illustrated in Figure [4.4]. Here we can observe that reducing w_1 from 1000 to 10, and from 10 to 0.1 gradually decreases the rate of false positives up to a limiting curve given as

$$\lim_{w_1 \to 0+} p_\infty(b^-) = \max\left[T + \frac{a^- + b^-}{a^- + b_T^-}(c_N - T_T), 0\right].$$

Note that in a natural system, the rates of communication would be limited by their physical bounds, and the optimal solution would lie on the physical boundary. Even then, we would be trading a very low chance of false positives for a very long activation time. A similar problem of infinite activation times in constrained minimization of false positives was encountered in changes of dissociation rate and heterogeneous networks suggesting activation time needs to be considered in optimization.

4.3 Optimization of Time Performance

As was shown above, minimization of false positives in the interesting biological cases without taking time performance into account leads to infinite activation times. Time performance cannot be neglected and the optimization problem must be redefined to include the activation time. An important

question is again how to measure the time performance? Several different metrics already exist and are commonplace in control theory. Often, integral criterions such as ITAE, ITE and ISE are used in controller design. Furthermore, system's eigenvalues (or linearized system's eigenvalues, or metrics using eigenvalues indirectly, such as linearized system matrix trace, etc. are used to measure time properties of the controlled system. Several of the above mentioned metrics were tested. Linearization and eigenvalue approach did not lead to useful results. Of the integral criterions, ITAE proved to be solvable even for induced activation, yet after careful analysis, it was shown the resulting criterion is for some parameter values non convex and the globally optimal design would be difficult to find. Lastly, simply the activation time was considered. It proved to be solvable in all cases, and convex for all relevant parameter values. The sections below explain the choice of criterion, the solution to the optimization problem and discuss the obtained optimal designs.

4.3.1 Criterion

The minimized quantity is the time the system requires to reach a given level of activity p_C at target, i.e., $b^- = b_T^-$ from the initial condition $p(0) = 0$, given as

$$p(t_{crit}) = p_C. \tag{4.17}$$

To compare the different biological cases, equal steady state activity at target c_N, resp. steady state activity at background c_P between compared designs must be enforced, i.e.,

$$p_\infty|_{b^-=b_T^-} = c_N, \tag{4.18}$$

$$p_\infty|_{b^-=\Delta b_T^-} = c_P. \tag{4.19}$$

The critical level of activity p_C can then be measured as a ratio R of the steady state value c_N such that

$$p_C = R p_\infty|_{b^-=b_T^-} = R c_N, \tag{4.20}$$

which reduces Equation [4.17] to

$$p(t_{crit}) = R c_N. \tag{4.21}$$

The criterion takes two forms depending on the linearity of the underlying differential equation.

Linear Case

In the linear case, the criterion is computed as follows

$$p_C = Rp_\infty = p_\infty(1 - e^{bt_{crit}}),$$
$$t_{crit} = \frac{1}{b}\log[1 - R].$$

Since b has is smaller than zero, it is more practical to write the criterion as follows

$$t_{crit} = -\frac{1}{b}\log\left[\frac{1}{1-R}\right]. \tag{4.22}$$

Without proof, we see that the criterion is convex, as b is an affine function of free parameters. Note that minimization of t_{crit} is equal to maximizing $-b$. Since $-b$ is an affine function of free parameters, we can predict that the optimal parameter values will lie on the boundary, which is given by the physical limits on free parameters.

Nonlinear Case

In the non-linear case, the criterion t_{crit} is computed from

$$p(t_{crit}) = (1 - \frac{p_\infty - p_\infty^*}{p_\infty - p_\infty^* \exp[b' t_{crit}]})p_\infty = p_C$$

as follows

$$t_{crit} = \frac{1}{b'}\log\left[-\frac{p_C - p_\infty^*}{p_\infty - p_C}\frac{p_\infty}{p_\infty^*}\right] = \frac{1}{a(p_\infty^* - p_\infty)}\log\left[-\frac{p_C - p_\infty^*}{p_\infty - p_C}\frac{p_\infty}{p_\infty^*}\right].$$

If the critical activity p_C is measured in terms of c_N such that

$$p_C = Rp_\infty|_{b^- = b_T^-} = Rc_N$$

then

$$t_{crit} = \frac{1}{a(p_\infty^* - p_\infty)}\log\left[\frac{1}{1-R}\left(1 - R\frac{p_\infty}{p_\infty^*}\right)\right]. \tag{4.23}$$

Furthermore, it may be derived that

$$t_{crit} = \frac{1}{-b - 2ap_\infty}\log\left[\frac{1}{1-R}(1 + R + R\frac{b}{c}p_\infty)\right]. \tag{4.24}$$

4.3.2 Case Studies Solution

Below, the optimization problem defined above is solved for three biologically relevant subcases of general one step activation, defined in Section [3.3.3]. For each design, the optimal solution is derived and its feasibility is discussed. The optimal design is then shown in two important plots: a) steady state activity $p_2(b^-)$ as a function of b^-. b) time response of the system $p_2(t)$

4.3.3 Spontaneous Activation

Under spontaneous activation, Equation [3.16] reduces to the following linear differential equation

$$\frac{dp(t)}{dt} = a^+ T_\infty - (a^+ + a^- + b^-)p(t) \quad p(0) = 0 \tag{4.25}$$

the solution of which is

$$p(t) = \frac{a^+ T_\infty}{a^+ + a^- + b^-} \left(1 - \exp\left[-(a^+ + a^- + b^-)t\right]\right). \tag{4.26}$$

The criterion is derived from Equation [4.22] as

$$J = t_{crit} = \frac{1}{a^+ + a^- + b_T^-} \log\left[\frac{1}{1-R}\right]. \tag{4.27}$$

The problem is constrained by the constraints on false positives and false negatives

$$p_\infty\Big|_{b^- = b_T^-} = \frac{a^+ T_T}{a^+ + a^- + b_T^-} = c_N, \tag{4.28}$$

$$p_\infty\Big|_{b^- = \Delta b_T^-} = \frac{a^+ T_B}{a^+ + a^- + \Delta b_T^-} = c_P, \tag{4.29}$$

which may be rewritten as

$$a^+ - \Gamma_N a^- = \Gamma_N b_T^-, \tag{4.30}$$

$$a^+ - \Gamma_P a^- = \Delta\Gamma_P b_T^-. \tag{4.31}$$

This system of linear equations has the following solution

$$a^+ = \Gamma_N \Gamma_P \frac{\Delta - 1}{\Gamma_N - \Gamma_P} b_T^-, \tag{4.32}$$

$$a^- = \frac{\Delta\Gamma_P - \Gamma_N}{\Gamma_N - \Gamma_P} b_T^-. \tag{4.33}$$

Interestingly, the parameters are linearly dependent on b_T^-. We see that is is possible to introduce a dimensionless problem by defining $\alpha^+ = \frac{a^+}{b_T^-}$ and $\alpha^- = \frac{a^-}{b_T^-}$. We will see that this holds in the other cases as well.

Once the solution to the constraints is known, there is no free parameter to optimize, therefore the optimization problem is solved. From this, the steady state activity can be computed as

$$p_\infty(b^-) = \frac{\Gamma_N \Gamma_P (\Delta - 1)}{\Gamma_N \Gamma_P (\Delta - 1) + \Delta\Gamma_P - \Gamma_N + (\Gamma_N - \Gamma_P)\frac{b^-}{b_T^-}} \frac{b^+}{b^+ + b^-} \tag{4.34}$$

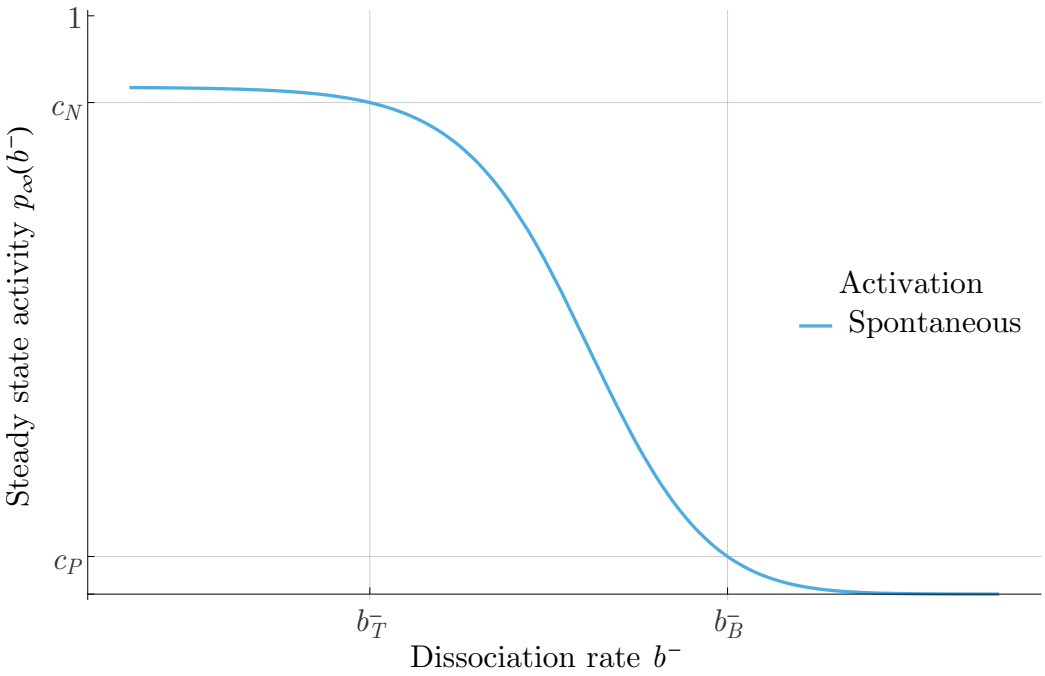

Figure 4.5: Steady state activity p_∞ of the optimal spontaneous activation as a function of dissociation rate b^-.

Which is illustrated in the following Figure [4.5] by the blue curve. As we can see, spontaneous activation produces a sigmoidal activation curve across different dissociation rates. The activity at target is fixed at c_N and at background at c_P, as was defined by the optimization constraints. The constraints are however not always achievable. The free parameters a^+ and a^- are required to be nonnegative, i.e., $a^+ \geq 0 \wedge a^- \geq 0$. By investigating signs of a^+ and a^- from Equation [4.32] and Equation [4.33] w.r.t. Γ_N and Γ_T we find that the constraints are feasible only if

$$\Gamma_N > \Gamma_P \geq \frac{\Gamma_N}{\Delta}. \tag{4.35}$$

The first condition can be rewritten in terms of original variables

$$c_P < \frac{T_B}{T_T} c_N = c_P^{\max} = \frac{b^+ + b_T^-}{b^+ + \Delta b_T^-} c_N. \tag{4.36}$$

This constraint says the problem is unfeasible if the ratio of active to total bound at background is equal to or greater than the same ratio at target. This is only natural as we require the ratio of active to total bound to be much smaller at background than at target. Case $\Gamma_N = \Gamma_P$ is physically

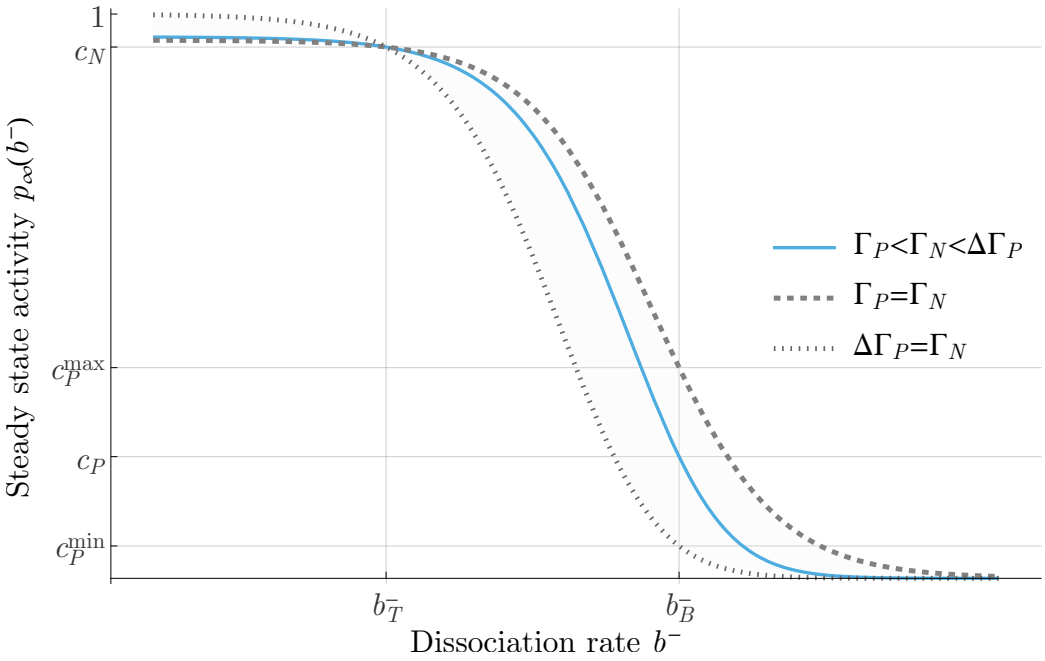

Figure 4.6: Feasibility of the optimization constraints for spontaneous activation.

irrelevant and therefore not discussed. The second condition may not be rewritten as

$$c_P \geq \frac{T_B}{\Delta T_T - \Delta c_N + c_N} c_N = c_P^{min} = \tag{4.37}$$
$$= \frac{b^+}{(b^+(c_N(\Delta-1)-\Delta) + b_T^- c_N(\Delta-1))} c_P^{max}$$

and is difficult to physically interpret.

The limits are illustrated in the Figure [4.6]. The dot-dashed line, i.e., the curve that corresponds to the lower bound of false positives c_P^{min}, is the solution when $a^- = 0$, The dashed line, which gives the upper bound on false positives c_P^{max}, corresponds to the solution when $a^+ \to \infty$ and $a^- \to \infty$. Both of these curves are in agreement with the limiting curves obtained in Section [4.2.1] in minimization of false positives. The blue curve corresponds to a solution in the feasible false positive domain. Once we obtained the (optimal) parameter values, we can compute the minimal value of the criterion J_0 from Equation [4.27] as

$$J_0 = \min_{a^+,a^-} J = \frac{1}{\Delta - 1} \frac{1}{\Gamma_N + 1} \frac{1}{b_T^-} \frac{\Gamma_N - \Gamma_P}{\Gamma_P} \log\left[\frac{1}{1-R}\right]. \tag{4.38}$$

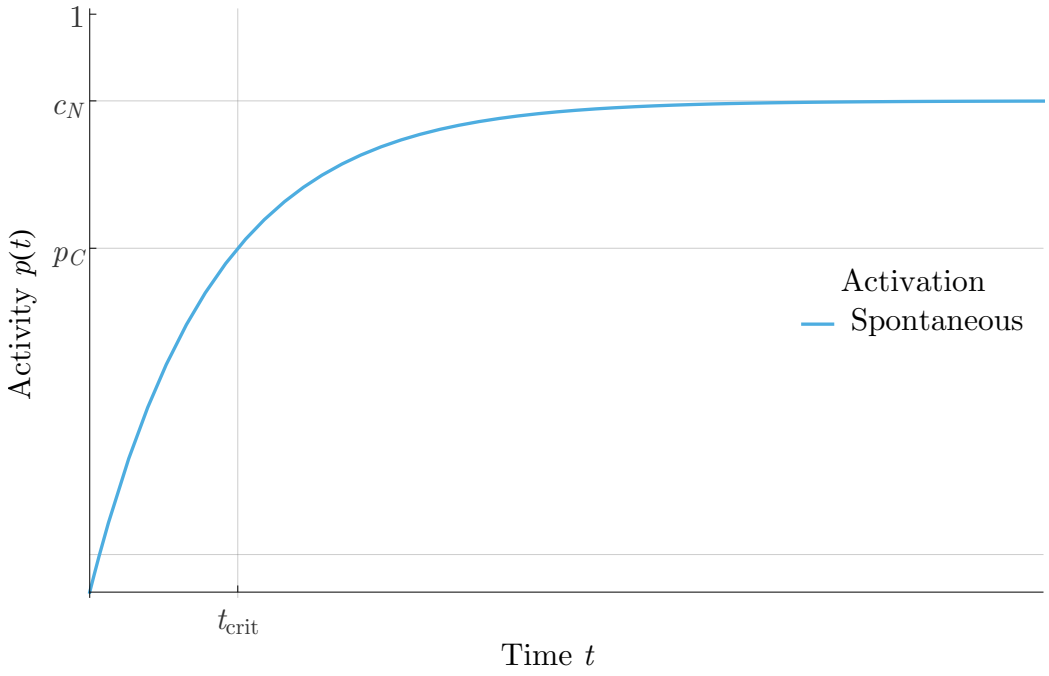

Figure 4.7: Activity time response $p(t)$ for the optimal spontaneous activation.

The time response at target is then

$$p(t) = c_N \left(1 - \exp\left[-\frac{\Gamma_N + 1}{\Gamma_N - \Gamma_P}\Gamma_P(\Delta - 1)b_T^- t\right]\right). \tag{4.39}$$

The time response is illustrated in the Figure [4.7] by the blue curve. As a solution to a first degree linear differential equation, it an exponential, upward curved from initial condition $p(0) = 0$ to the steady state condition $p_\infty = c_N$.

4.3.4 Constitutive Activation

Under constitutive activation, the system is described by the following linear differential equation

$$\frac{dp(t)}{dt} = (a^+ + wT_\infty)T_\infty - (a^+ + a^- + b^- + wT_\infty)p(t) \tag{4.40}$$

the solution of which (from Equation [3.20]) is

$$p(t) = \frac{a^+ + wT_\infty}{a^- + b^- + wT_\infty} T_\infty \left(1 - \exp\left[-(a^+ + a^- + b^- + wT_\infty)t\right]\right). \tag{4.41}$$

The criterion is (from Equation[4.22]) defined as

$$J = t_{crit} = \frac{1}{a^+ + a^- + b_T^- + wT_T} \log\left[\frac{1}{1-R}\right]. \tag{4.42}$$

The optimization constraints take the form of

$$p_\infty\Big|_{b^-=b_T^-} = \frac{a^+ + wT_T}{a^+ + a^- + b_T^- + wT_T} = \frac{c_N}{T_T}, \tag{4.43}$$

$$p_\infty\Big|_{b^-=\Delta b_T^-} = \frac{a^+ + wT_B}{a^+ + a^- + \Delta b_T^- + wT_B} = \frac{c_P}{T_B}. \tag{4.44}$$

Equation [4.43] and Equation [4.44] are more easily solvable with the use of variables Γ_N and Γ_P (see Section [4.2]) as

$$a^+ - \Gamma_N a^- + T_T w = \Gamma_N b_T^-, \tag{4.45}$$

$$a^+ - \Gamma_P a^- + T_B w = \Delta\Gamma_P b_T^- \tag{4.46}$$

By solving Equation [4.30] and Equation [4.46], we obtain

$$a^- = \frac{\Delta\Gamma_P - \Gamma_N}{\Gamma_N - \Gamma_P} b_T^- + \frac{T_T - T_B}{\Gamma_N - \Gamma_P} w, \tag{4.47}$$

$$a^+ = \Gamma_N\Gamma_P \frac{\Delta - 1}{\Gamma_N - \Gamma_P} b_T^- - \frac{T_B\Gamma_N - T_T\Gamma_P}{\Gamma_N - \Gamma_P} w. \tag{4.48}$$

Note that again, one could define a dimensionless parameters $\omega = \frac{w}{b_T^-}, \alpha^+ = \frac{a^+}{b_T^-}$, and $\alpha^- = \frac{a^-}{b_T^-}$ to define a dimensionless problem as we saw in Section [4.3.3]. By substituting the solution [4.47] and into the criterion Equation [4.42], we obtain

$$J_1 = \frac{1}{\Gamma_N + 1} \frac{\Gamma_N - \Gamma_P}{(\Delta - 1)\Gamma_P b_T^- + (T_T - T_B)w} \log\left[\frac{1}{1-R}\right]. \tag{4.49}$$

Since $T_T > T_B$, the criterion J decreases as w increases, therefore, to minimize the criterion, W should be set to its maximal value, which is determined from the physical constraints. As we saw in previous Section [4.3.3], the feasibility of the problem largely depends on the relationship of Γ_N and Γ_P. By analysis of Equation [4.47] and [4.48], we learn that there are five important cases determined by the relation between the value of Γ_N w.r.t. four critical values $\left[\Delta\frac{T_T}{T_B}\Gamma_P, \Delta\Gamma_P, \frac{T_T}{T_B}\Gamma_P, \Gamma_P\right]$. All possible cases are discussed in the table below.

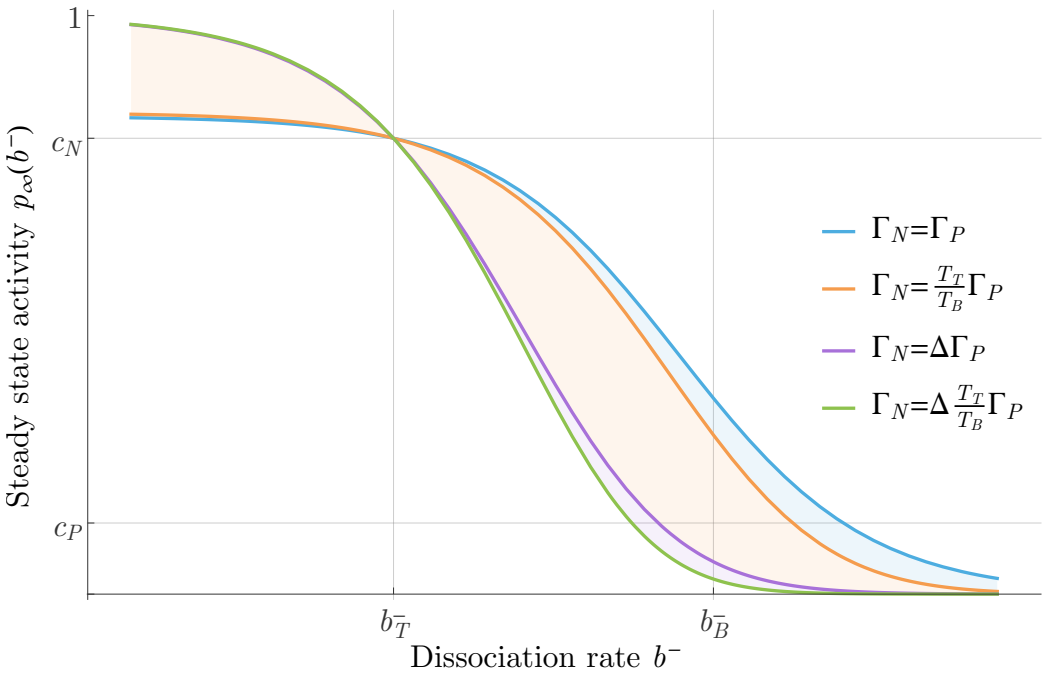

Figure 4.8: Steady state activity p_∞ as a function of dissociation rate b^- for the four limiting cases of constitutive activation.

Case	Limits	Comments
1	$\Gamma_P \geq \Gamma_N$	Unsolvable, physically irrelevant.
2	$\frac{T_T}{T_B}\Gamma_P > \Gamma_N > \Gamma_P$	Solvable, w is constrained only by the physical constraint, not discussed below.
3	$\Delta\Gamma_P > \Gamma_N > \frac{T_T}{T_B}\Gamma_P$.	Solvable, $w \in [0, w_{max}]$, where w_{max} is determined from $a^+ = 0$
4	$\Delta\frac{T_T}{T_B} \geq \Gamma_N > \Delta\Gamma_P$.	Solvable, $w \in [w_{min}, w_{max}]$, where w_{max} is determined from $a^+ = 0$, and w_{min} from $a^- = 0$.
5	$\Gamma_N > \Delta\frac{T_T}{T_B}\Gamma_P$	Unsolvable.

The cases are illustrated in Figure [4.8]. The four limiting curves are shown. The light blue area represents case 2), the orange area case 3), and the light purple case 4)

For cases 3) and 4), the optimal value $w^* = w_{\max}$ is therefore is determined from $a^+ = 0$ as

$$w_{\max} = \frac{\Delta - 1}{T_B\Gamma_N - T_T\Gamma_P}\Gamma_N\Gamma_P b_T^-. \tag{4.50}$$

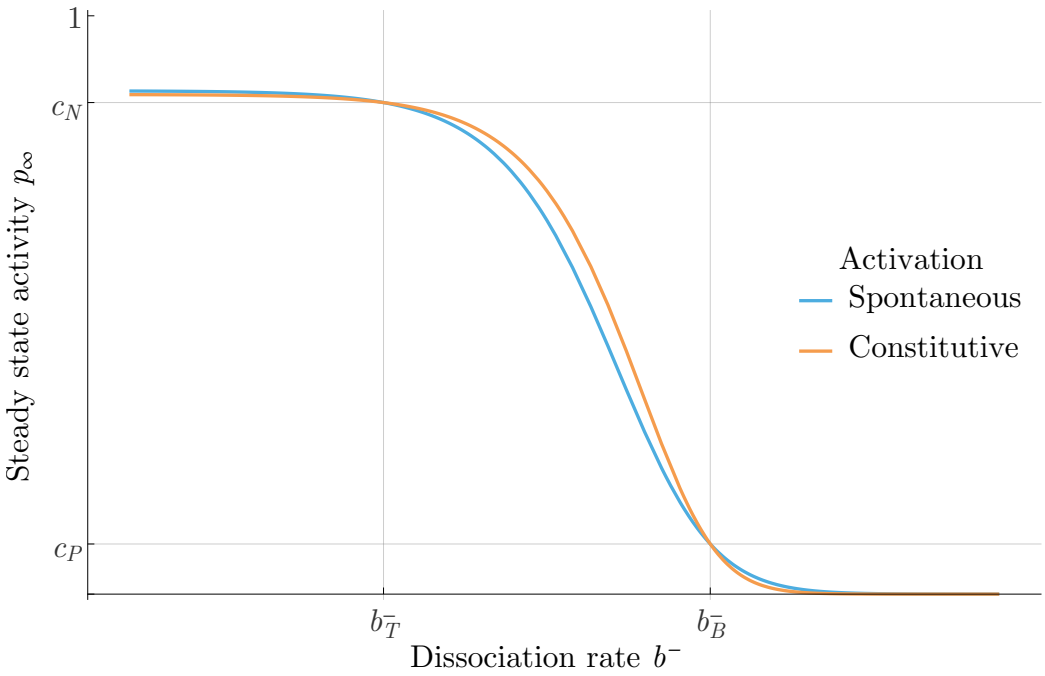

Figure 4.9: Steady state activity $p_\infty(b^-)$ as a function of dissociation rate b^- for the optimal constitutive activation.

After substitution of the optimal value of $w^* = w_{\max}$ back into the criterion Equation [4.49], we obtain

$$J_1 = \min_{a^+,a^-,w} J = \frac{1}{\Gamma_N + 1}\frac{1}{\Delta - 1}\frac{T_B\Gamma_N - T_T\Gamma_P}{T_T\Gamma_P b_T^-}\log\left[\frac{1}{1-R}\right]. \tag{4.51}$$

Equation [4.51] may be rewritten in terms of J_0 from Equation [4.38] as

$$J_1 = J_0\frac{T_B\Gamma_N - T_T\Gamma_P}{T_T(\Gamma_N - \Gamma_P)} = J_0\left(1 - \frac{\Gamma_N}{T_T}\frac{T_T - T_B}{\Gamma_N - \Gamma_P}\right). \tag{4.52}$$

5 From Equation, it is plain to see that $J_1 \leq J_0$, and $J_1 = J_0$ only if $\Gamma_N = \frac{T_T}{T_B}\Gamma_P$, therefore constitutive activation is always better than spontaneous. After the optimal parameter values are known, the design characteristics may be computed, starting with the steady state activity

$$p_\infty(b^-) = \frac{\Gamma_N\Gamma_P(\Delta - 1)}{\Delta T_T\Gamma_P + (T_B\Gamma_N - T_T\Gamma_P)\frac{b^-}{b_T^-} + \Gamma_N\Gamma_P(\Delta - 1)T}\left(\frac{b^+}{b^+ + b^-}\right)^2$$

The activity is illustrated in the figure below

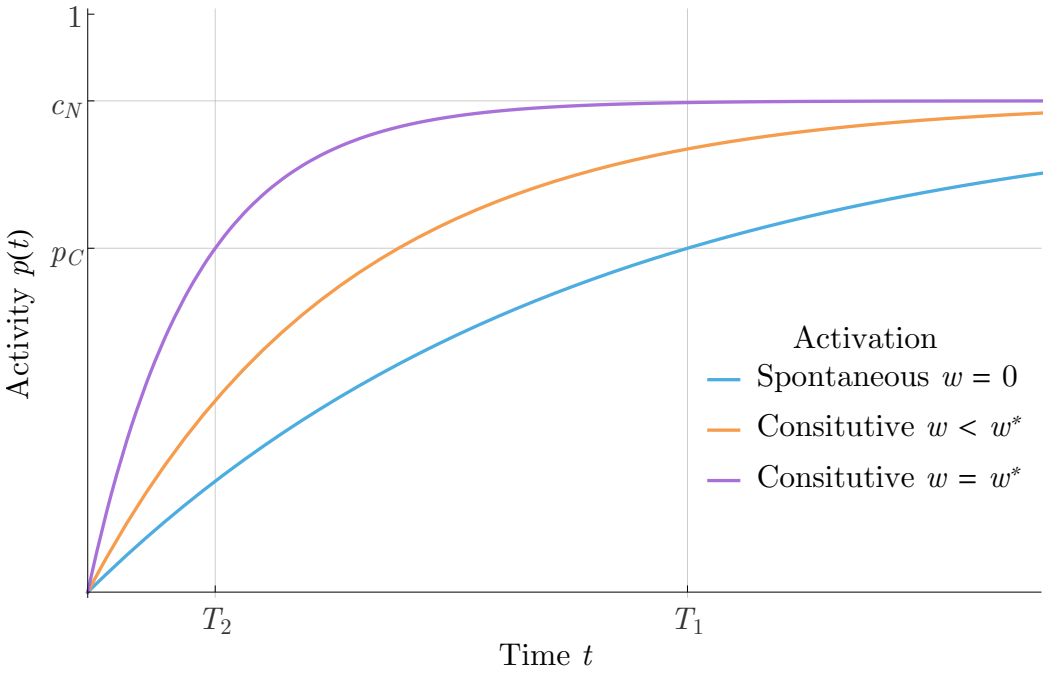

Figure 4.10: Activity responses $p(t)$ in time for the optimal spontaneous, sub-optimal constitutive and optimal constitutive activation.

From Equation [4.41], the time response is

$$p(t) = c_N \left(1 - \exp\left[-\left(\frac{(\Delta-1)\Gamma_P}{\Gamma_N - \Gamma_P} b_T^- + \frac{T_T - T_B}{\Gamma_N - \Gamma_P} w\right)(\Gamma_N + 1)t\right]\right) \quad (4.53)$$

For optimal $w^* = w_{max}$, Equation [4.53] reduces to

$$p(t) = c_N \left(1 - \exp\left[-\frac{T_T \Gamma_P}{T_B \Gamma_N - T_T \Gamma_P}(\Delta - 1)(\Gamma_N + 1) b_T^- t\right]\right) \quad (4.54)$$

The time behavior of the system is illustrated in the Figure [4.10] below.

4.3.5 Induced Activation

Under induced activation, the general model in 3.16 doesn't reduce, i.e.,

$$\begin{aligned}\frac{dp}{dt} &= (a^+ + w_1 T_\infty)T_\infty - (a^+ + a^- + 2w_1 T_\infty - w_2 T_\infty + b^-)p \\ &\quad - (w_2 - w_1)p^2. \end{aligned} \quad (4.55)$$

The optimization constraints are given as

$$(a^+ + w_1 T_T)T_T - (a^+ + a^- + b_T^- + 2w_1 T_T - w_2 T_T)c_N - (w_2 - w_1)c_N^2 = 0,$$
$$(a^+ + w_1 T_B)T_B - (a^+ + a^- + b_B^- + 2w_1 T_B - w_2 T_B)c_P - (w_2 - w_1)c_P^2 = 0.$$

For the purpose of this section, it is useful to introduce the activation rate difference $W = w_2 - w_1$, as a difference between the activation rate of active and inactive sensor cells. Higher W results in higher use of positive feedback after activation. To simplify the derivations, we also introduce a dummy variable

$$A = a^- + b_T^-$$

Then the optimization constraints may be rewritten as

$$a^+ = \Gamma_N A - T_T w_1 - c_N W, \tag{4.56}$$
$$a^+ = (\Delta - 1)\Gamma_P b_T^- + \Gamma_P A - T_B w_1 - c_P W. \tag{4.57}$$

The criterion can then be computed from Equation [4.24] as

$$J = \frac{1}{-b - 2ac_N} \log \left[\frac{1}{1-R} \frac{1 + Rac_N}{b + ac_N} \right] \tag{4.58}$$

where

$$\begin{aligned} c &= (a^+ + w_1 T_T)T_T = (\Gamma_N A - c_N W)T_T, \\ a &= -W, \\ b &= -\left(\frac{c(b_T^-)}{T_T} + A - WT_T \right) = -((\Gamma_N + 1)A - W(T_T + c_N)), \end{aligned}$$

which results in

$$J = \frac{1}{(\Gamma_N + 1)A - \frac{WT_T}{\Gamma_N + 1}} \log \left[\frac{1}{1-R} \left(1 + R \frac{\frac{Wc_N}{\Gamma_N + 1}}{A - \frac{WT_T}{\Gamma_N + 1}} \right) \right] \tag{4.59}$$

where A depends on W as

$$\frac{WT_T}{\Gamma_N + 1} = \frac{1}{T_B} \frac{\Gamma_P + 1}{\Gamma_N - \Gamma_P} \left[(T_T - T_B)a^+ - T_T(\Delta - 1)\Gamma_P b_T^- + (T_B\Gamma_N - T_T\Gamma_P)A \right]. \tag{4.60}$$

This criterion is convex, and the proof is given in Appendix [5]. It is easy to show that the criterion is always increasing in a^+, implying that $a^+ = 0$ is optimal. That is, communication, either from active or inactive cell is always preferred to spontaneous activation. The criterion is shown in Figure [4.11]. As expected, the criterion is convex in W and has a clear single minimum $W \in [0, W_{\max}]$. where $W_{\max}$ is given from the condition

$$(\Gamma_N + 1)A - \frac{WT_T}{\Gamma_N + 1} \geq 0 \tag{4.61}$$

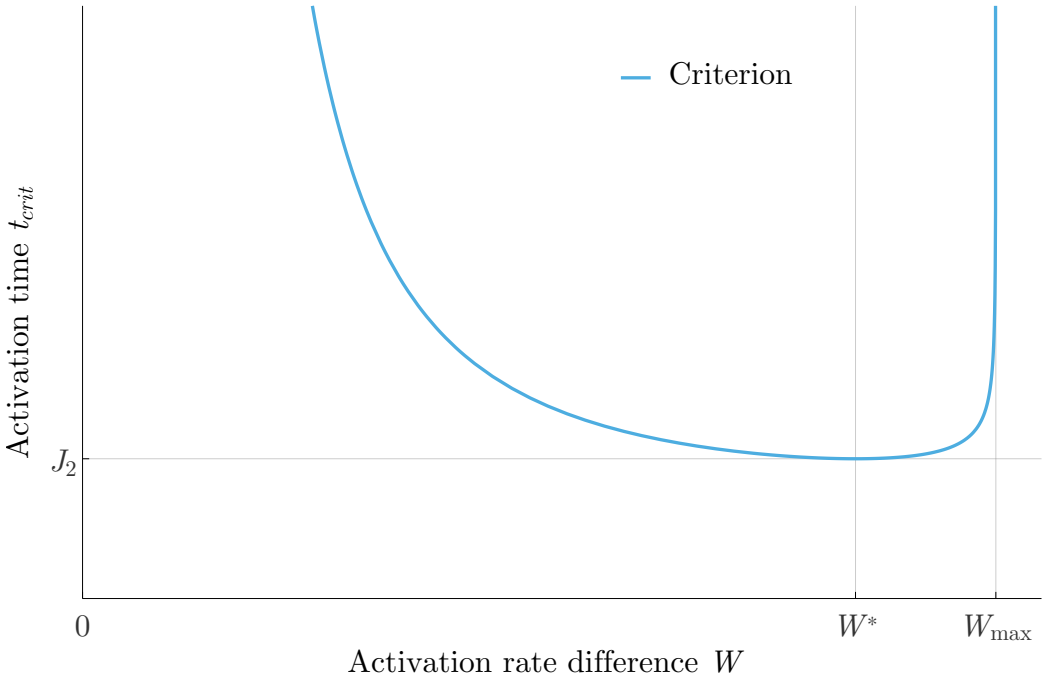

Figure 4.11: Activation time t_{crit} (criterion) for induced activation as a function of the activation rate difference W.

As convex, the criterion is guaranteed to have a single local minimum that is also global. This optimal point cannot be expressed analytically, however it can be found numerically. In this work, the optimal point was found using Mathematica software [14]. Figure [4.12] shows the optimal time responses of the three studied case for a chosen R. Compared to its counterparts, the optimal time response of induced activation has an inflection point.

Time responses of induced activation differ greatly for different values of activation rate difference W. This is summarized in Figure [4.13]. We see that as W increases, the response rises from below the constitutive activation response and the activation time decrease, until an optimal W^* is reached. For $W > W^*$, the activation time quickly increases. This is in agreement with the criterion graph in Figure [4.11]. Note the appearance of an inflection point as W increases.

Naturally, we could study the impact of each of parameters $\left\{b^+, b_T^-, \Delta, c_P, c_N, R\right\}$ on the optimal value of W and the minimal value of activation time t_{crit}. These impacts were tested but were often quite predictable, such as lower rate of false positives c_P results in longer activation times, and higher target/background marker difference Δ results in shorter activation times. Biologically, the most interesting is the impact of the desired value R. The optimization problem was defined so that the minimized

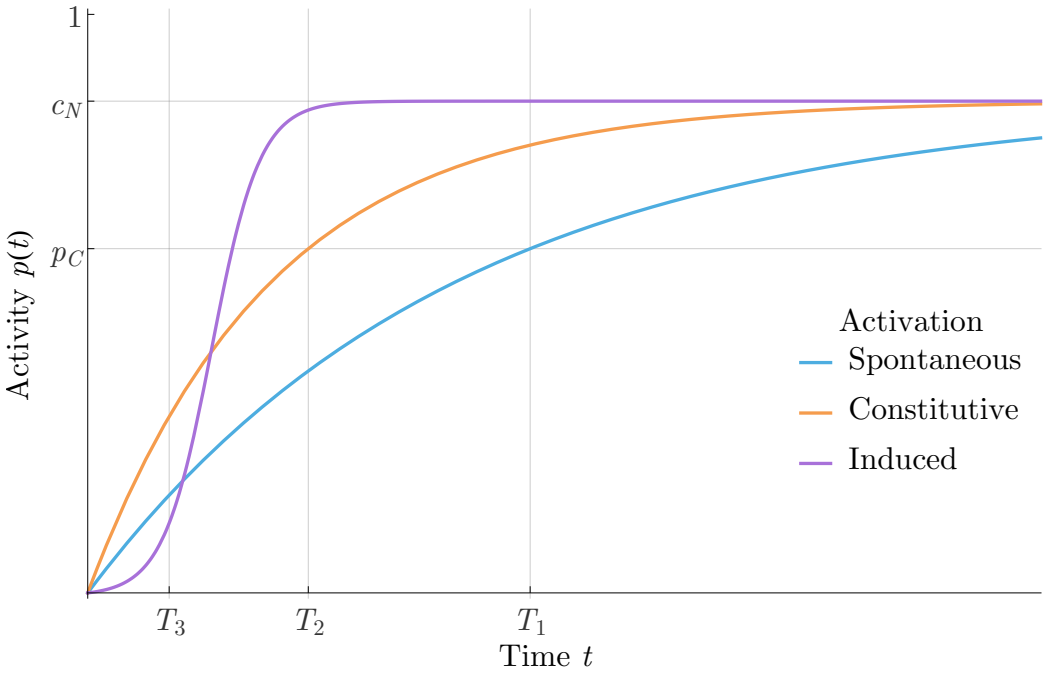

Figure 4.12: Activity time response $p(t)$ for the optimal spontaneous, optimal constitutive, and optimal induced activation.

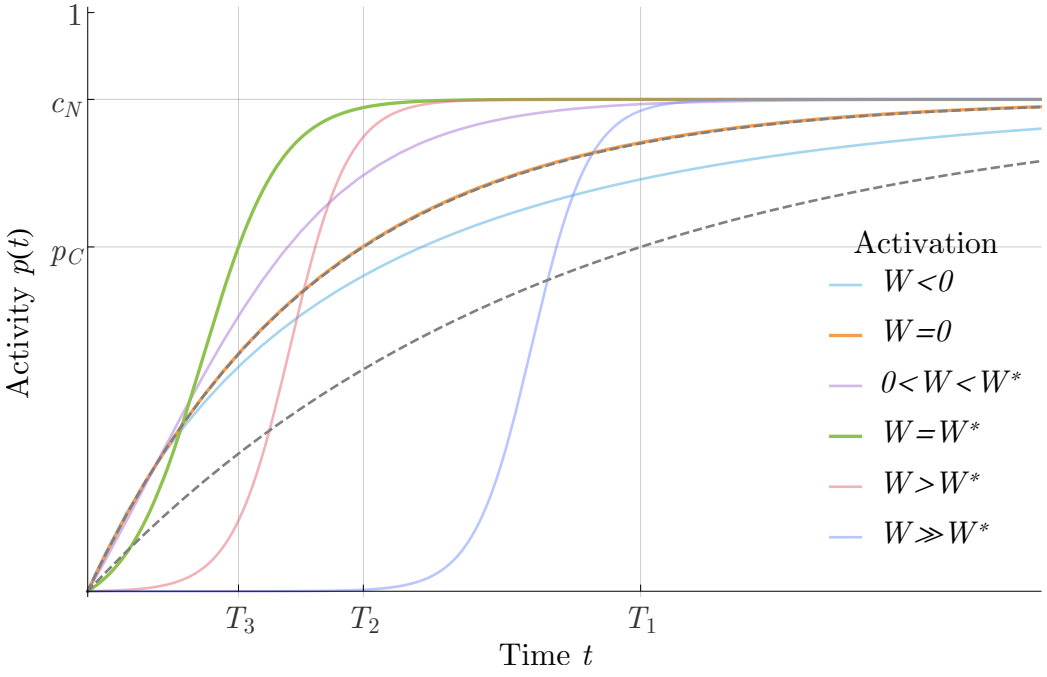

Figure 4.13: Overview of different options for activity time response $p(t)$ of induced activation for different activation rate difference W.

activation time is the time to reach percentage R of the steady state activity c_N. Reaching the critical percentage level can trigger a population wide biological change. Naturally, this critical rate of activity can be different for different changes, depending on the corresponding risk. Naturally, on one hand,for biologically costly changes the population needs to be sufficiently high before triggering the change to ensure no incorrect and detrimental activation. On the other hand, some changes are relatively cheap, and can be made based on a lower rate of activity. In both cases the decisions are required to be made as quickly as possible. We hypothesize that different cells use different activation values based on the triggered biological changes and their corresponding risk.

The impact of R on the solution to the optimization problem is described below. Results were obtained numerically by Mathematica [14], as the problem is analytically unsolvable, therefore no formulas are given. The impact on the activation time is shown in Figure [4.14]. For three different levels (low, medium, high) of desired activation R, the activation time is plotted against the communication difference W. Different desired activity results in different minimal time and different optimal communication rate difference $W^*(R)$. The curve that connects all optimal $W^*(R)$ against the minimal activation time for different R (increasing from $R = 0$ at $W = 0$) is plotted as the gray line. We see that as R increases, so does the minimal activation time, slowly at the start but more noticeably after $R = 0.2$. The curve then turns strongly upwards for $R > 0.8$ before reaching $W_{\max}$, suggesting that $\lim_{R\to 1} W^*(R) \neq W_{\max}$, i.e, small basal activation rates are required even for $R \to 1$.

The most interesting is the impact of R on the optimal activation difference rate $W^*(R)$. We see that as R increase, so does $W^*(R)$, i.e., for higher R the default rate w_1 should be set low and the feedback rate w_2 should be set high. This means that for biological changes with a low trigger threshold, positive feedback is not beneficial, whereas for problems with a higher threshold, it is needed, and more the higher the threshold.

For example, bacteria *Staphylococcus aureus* commonly creates skin infections in damp parts of the body, such as armpits. The secretion of virulence factors is largely controlled by *agr* QS system [15]. The corresponding constitutive expression rate of the communication molecule is estimated as 1.10^4 nM h^{-1} [6]. Bacteria *Pseudomonas aeruginosa* often invades bloodstream and uses the *las* QS system for its virulence factors [16]. The corresponding constitutive expression rate of the communication molecule is estimated as $3.10^3\,\mathrm{nM\,h^{-1}}$ [6]. We see that the constitutive expression rate is smaller for *Pseudomonas aeruginosa* since it invades a much harsher environment (blood), therefore it needs relatively high cell densities before deciding to start infection. *Staphylococcus aureus* lives in relatively favorable condi-

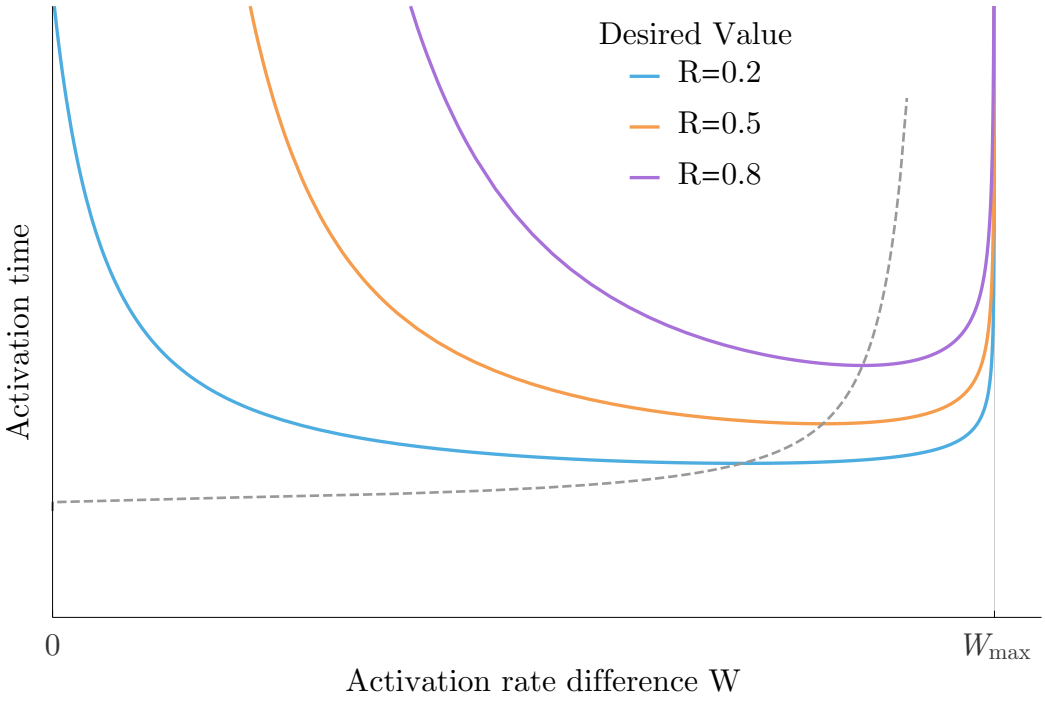

Figure 4.14: Impact of different desired value R on the relationship between activation and the activation rate difference W.

tions, therefore it triggers biofilm formation even at lower cell density and doesn't need to use feedback activation as much. Unfortunately feedback activation rates of these QS systems are not known.

The impact of R on the time response is summarized in the Figure [4.15] where optimal responses of induced activation for different desired activations R are shown. Higher R results in a stronger feedback loop, therefore slower activation at the start but much quicker at the end. For the lower $R = 0.2$, the response resembles that of constitutive activation, as feedback is used only weakly.

4.3.6 False Positives Impact

Above, the designs yielding minimal activation time were presented for three biologically relevant cases. The designs were compared in steady state activity and time response. These designs can be compared from another perspective. Consider we keep the constraint c_N on false positives equal among the different designs, but we change the constraint. This is equivalent to resolving the optimization problem with a constraint on time and background steady state activity as the criterion. One can then obtain analytic results for spontaneous and constitutive activation, however, for induced activation only numerical results may be obtained. Consider that the background

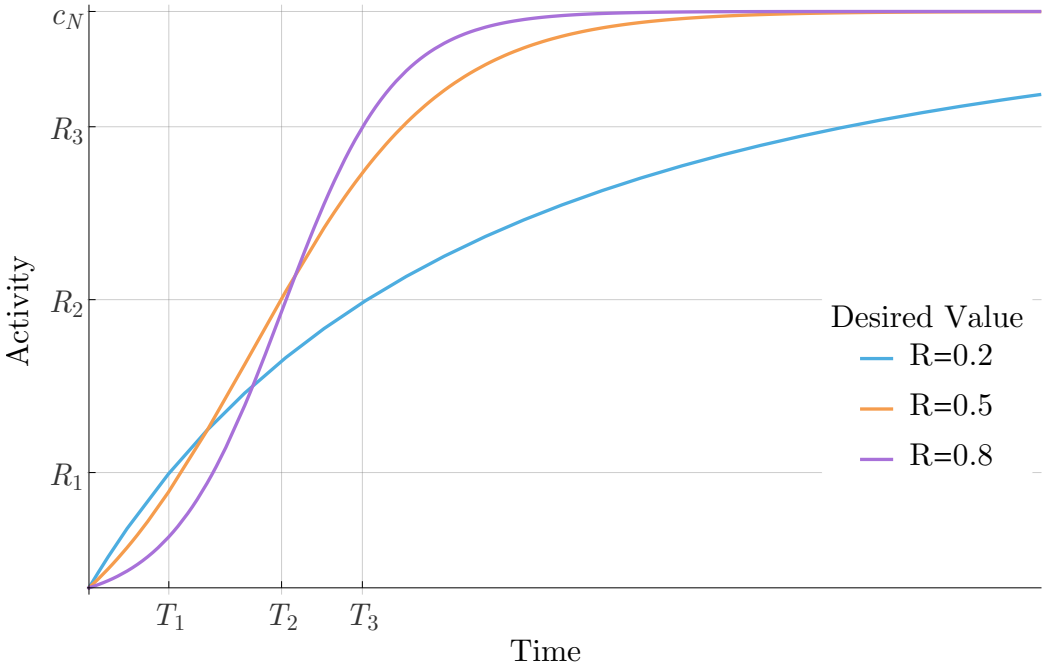

Figure 4.15: Overview of different options for activity time response $p(t)$ of optimal induced activation for desired values R.

steady state activity is $c_P = c_{P,1} \rightarrow \Gamma_P = \frac{c_{P,1}}{T_T - c_{P,1}}$ for spontaneous activation and $c_P = c_{P,2} \rightarrow \Gamma_P = \frac{c_{P,2}}{T_T - c_{P,2}}$ for constitutive activation.

Activation	Criterion
Spontaneous	$J_0 = \frac{1}{\Gamma_N+1}\frac{1}{\Delta-1}\frac{1}{b_T^-}\frac{\Gamma_N-\Gamma_{P,1}}{\Gamma_{P,1}}\log\left[\frac{1}{1-R}\right]$
Constitutive	$J_1 = \frac{1}{\Gamma_N+1}\frac{1}{\Delta-1}\frac{1}{b_T^-}\frac{T_B\Gamma_N - T_T\Gamma_{P,2}}{T_T\Gamma_{P,2}}\log\left[\frac{1}{1-R}\right]$

We then determine $\Gamma_{P,2}$ that yields equal time of constitutive and spontaneous activation ($J_0 = J_1$)

$$\Gamma_{P,2} = \frac{T_B}{T_T}\Gamma_{P,1}. \tag{4.62}$$

Interestingly, the relation is independent of Γ_N. Equation [4.62] may be expressed in the original variables c_P and c_N

$$c_{P,2} = \frac{b^+(b^+ + b_T^-)c_{P,1}}{(b^+ - b_T^- c_{P,1}(\Delta-1))(b^+ + b_T^-\Delta)} = \frac{b^+}{b^+ - b_T^- c_P(\Delta-1)}c_P^{max}.$$

Again, the relation is independent of c_N. Furthermore, it can be derived that not only the critical time is equal between the designs, but also the time response.

Rate of false positives $\Gamma_{P,3}$, that yields equivalent activation time for induced activation may be computed by the same principles, yet only numerically. Note that the response of induced activation is then equal to those of constitutive/spontaneous activation only in one point.

Under these conditions on false positives, steady state activity curves can be computed for different activation types. These are illustrated in Figure [4.16]. We see that the different activation types are ordered as expected, with spontaneous activation (in blue) resulting in highest number of false positives and induced activation (in purple) resulting in in lowest rate of false positives. Note that difference between spontaneous and constitutive activation (in orange) is larger than the difference between induced and constitutive activation.

Interesting is also the graph of minimal activation time as a function of the constraint c_P on steady state background activity shown in Figure [4.17]. we again observe that the gap between constitutive and spontaneous activation is larger than that between induced and constitutive activation. Note that for higher values of c_P, determined by the bounds on solvability, which are $c_P^{\text{com}} : \Gamma_N = \frac{T_T}{T_B}\Delta\Gamma_P$ for induced and constitutive activation, and c_P^{max} for spontaneous activation, the activation time converges to zero. This is because we do not consider the physical bounds on parameters. In reality, there will be a nonzero minimal possible activation time, shown as a dashed line.

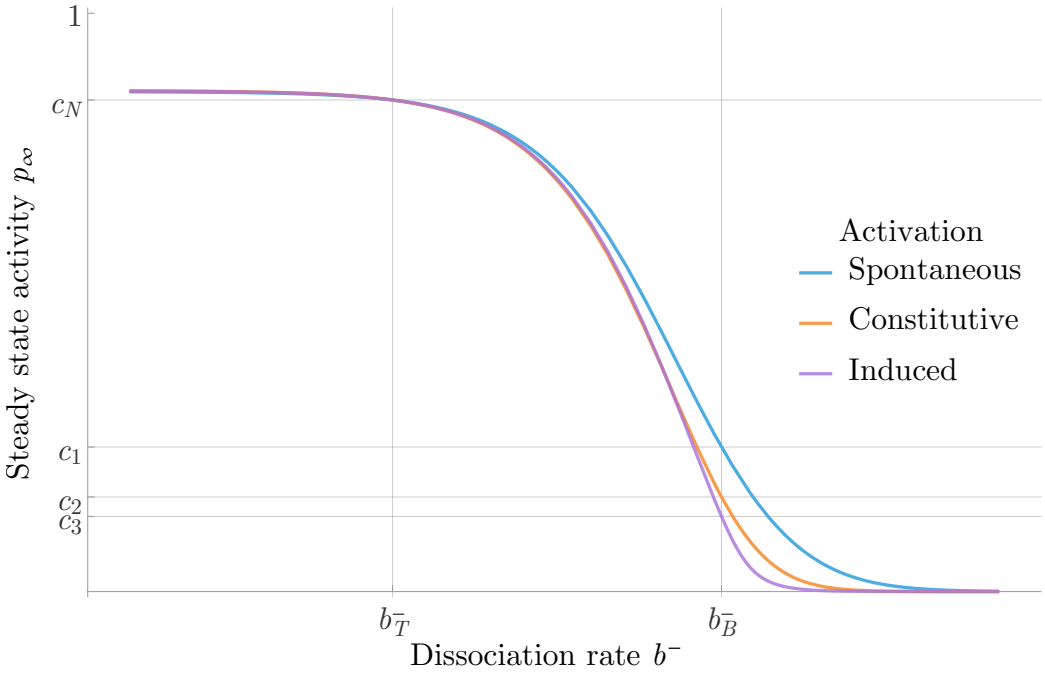

Figure 4.16: Steady state activity $p_\infty(b^-)$ for different activation designs with constraint c_P adjusted to equal activation time.

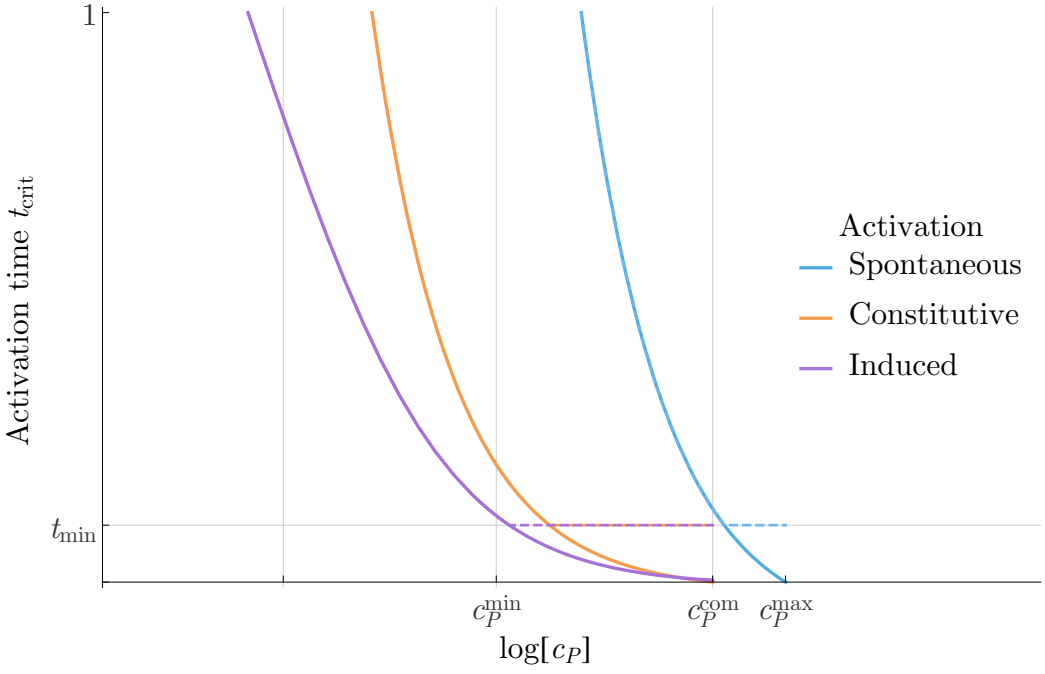

.

Figure 4.17: Minimal activation time of different activation designs as a function of steady state background activity constraint c_P.

5. Discussion

This work introduced a stochastic process based method for modelling of cell communication between co-localized cells. The need for simulation of complex communication networks was illustrated by presenting examples of known communication systems along with mathematical description. Strengths and weaknesses of the proposed method were stated, with the largest difference between the proposed method and other methods being ability to provide analytic results, and largest limitation being a specific, yet broad range of communication networks.

The potential of the proposed method was illustrated on a derivation of a model of homogeneous single marker communication network with one step activation, which represents a QS system. Performance of this network model was then optimized. Three biologically relevant cases of optimized network were considered including spontaneous, constitutive and induced activation. Firstly, it was shown that neglecting time performance provides unrealistic results. Secondly, constrained optimization including time performance was used to derive design rules yielding optimal performance for all three cases.

It was shown that spontaneous activation is never preferred over communication. Additionally, it was shown that induced activation generally provides the best performance of the three considered cases. The impact of the desired activity on the optimal solution was discussed. It was shown that for a higher desired activity, a stronger feedback activation is optimal. From this, a hypothesis was proposed that QS systems triggering a biological change at threshold concentration should be designed with feedback activation, the stronger the higher the threshold is. This hypothesis is supported by the common occurrence of positive feedback in QS systems and further supported by low rate of feedback activation for biofilm formation of bacteria living in favorable environments such as *Staphylococcus aureus* and higher rate of feedback activation for bacteria living in harsh conditions such as *Pseudomonas aeruginosa*.

Future work will focus on generalizing and extending some of the statements introduced in this text, testing the analytic results in more complex simulation environments, and using synthetic biology to verify obtained results in experiments.

A. Proof of criterion convexity

The criterion for activation time optimization is given as Equation [4.59]. One may then define a linear change of variables as follows

$$\begin{aligned}\kappa &= \frac{R}{1-R}\frac{1}{\Gamma_N+1}, \qquad \kappa > 0\\ Y &= (\Gamma_N+1)A - \frac{WT_T}{\Gamma_N+1}\\ Z &= \Gamma_N A,\end{aligned}$$

which reduces the criterion to

$$J(Y,Z) = \frac{1}{Y}\log\left[1+\frac{\kappa Y}{Y-Z}\right]. \tag{A.1}$$

By investigating the signs of variables w_1, w_2 w.r.t. Y and Z, we can derive that the solution has a physical meaning only if

$$Y > Z > 0. \tag{A.2}$$

The hessian of the criterion in Equation [A.1] is

$$\nabla^2 J = 2\kappa\frac{-2\kappa Y + (-2Z + Y(2+\kappa))\log\left[1+\frac{\kappa Y}{Y-Z}\right]}{Y^3(Y-Z)^2(Y-Z+Y\kappa)^2}. \tag{A.3}$$

The sign of hessian is determined by the nominator, as all other terms are strictly positive. More specifically, the hessian is positive if the nominator is positive

$$\log\left[1+\frac{\kappa Y}{Y-Z}\right] \geq \frac{2\kappa Y}{2(Y-Z)Z+\kappa Y}. \tag{A.4}$$

This can be proved by using inequality

$$\log[1+x] \geq \frac{2x}{2+x} \quad \forall x \geq 0 \tag{A.5}$$

from [17]. If one sets $x = \frac{\kappa Y}{Y-Z}$ it is plain to see that the inequality in Equation [A.4] holds for all feasible Y and Z, therefore the hessian in Equation [A.3] is positive. A positive hessian implies convexity.

Bibliography

[1] P. Williams, K. Winzer, W. C. Chan, and M. Cámara, "Look who's talking: communication and quorum sensing in the bacterial world," *Philosophical Transactions of the Royal Society B: Biological Sciences*, vol. 362, no. 1483, pp. 1119–1134, 2007.

[2] G. J. Lyon and R. P. Novick, "Peptide signaling in staphylococcus aureus and other gram-positive bacteria," *Peptides*, vol. 25, no. 9, pp. 1389 – 1403, 2004. M. Altstein.

[3] B. L. Bassler and R. Losick, "Bacterially speaking," *Cell*, vol. 125, no. 2, pp. 237 – 246, 2006.

[4] B. L. Bassler, "Small talk: Cell-to-cell communication in bacteria," *Cell*, vol. 109, no. 4, pp. 421 – 424, 2002.

[5] B. A. Lazazzera, I. G. Kurtser, R. S. McQuade, and A. D. Grossman, "An autoregulatory circuit affecting peptide signaling in bacillus subtilis," *Journal of bacteriology*, vol. 181, no. 17, pp. 5193–5200, 1999.

[6] A. Pai and L. You, "Optimal tuning of bacterial sensing potential," *Molecular Systems Biology*, vol. 5, no. 1, 2009.

[7] S. Netotea, I. Bertani, L. Steindler, Á. Kerényi, V. Venturi, and S. Pongor, "A simple model for the early events of quorum sensing in pseudomonas aeruginosa: modeling bacterial swarming as the movement of an "activation zone"," *Biology Direct*, vol. 4, no. 1, pp. 1–16, 2009.

[8] T. E. Gorochowski, A. Matyjaszkiewicz, T. Todd, N. Oak, K. Kowalska, S. Reid, K. T. Tsaneva-Atanasova, N. J. Savery, C. S. Grierson, and M. di Bernardo, "Bsim: An agent-based tool for modeling bacterial populations in systems and synthetic biology," *PLoS ONE*, vol. 7, pp. 1–9, 08 2012.

[9] P. Gerlee and A. Anderson, "A hybrid cellular automaton model of clonal evolution in cancer: The emergence of the glycolytic phenotype," *Journal of Theoretical Biology*, vol. 250, no. 4, pp. 705 – 722, 2008.

[10] C. Picioreanu, M. C. M. van Loosdrecht, and J. J. Heijnen, "A new combined differential-discrete cellular automaton approach for biofilm modeling: Application for growth in gel beads," *Biotechnology and Bioengineering*, vol. 57, no. 6, pp. 718–731, 1998.

[11] M. Mimura, H. Sakaguchi, and M. Matsushita, "Reaction–diffusion modelling of bacterial colony patterns," *Physica A: Statistical Mechanics and its Applications*, vol. 282, no. 1–2, pp. 283 – 303, 2000.

[12] K. Kawasaki, A. Mochizuki, M. Matsushita, T. Umeda, and N. Shigesada, "Modeling spatio-temporal patterns generated bybacillus subtilis," *Journal of Theoretical Biology*, vol. 188, no. 2, pp. 177 – 185, 1997.

[13] V. L. MacKay, S. K. Welch, M. Y. Insley, T. R. Manney, J. Holly, G. C. Saari, and M. L. Parker, "The saccharomyces cerevisiae bar1 gene encodes an exported protein with homology to pepsin," *Proceedings of the National Academy of Sciences*, vol. 85, no. 1, pp. 55–59, 1988.

[14] I. Wolfram Research, "Mathematica, version 10.4," 2016.

[15] N. Balaban and R. P. Novick, "Translation of rnaiii, the staphylococcus aureus agr regulatory rna molecule, can be activated by a 3'-end deletion," *FEMS Microbiology Letters*, vol. 133, no. 1-2, pp. 155–161, 1995.

[16] M. J. Kirisits and M. R. Parsek, "Does pseudomonas aeruginosa use intercellular signalling to build biofilm communities?," *Cellular Microbiology*, vol. 8, no. 12, pp. 1841–1849, 2006.

[17] F. Topsok, "Some bounds for the logarithmic function," *Inequality theory and applications*, vol. 4, p. 137, 2006.